Water Research 236 (2023) 119969

Contents lists available at ScienceDirect

Water Research

journal homepage: www.elsevier.com/locate/watres

Urban landscapes and legacy industry provide hotspots for riverine greenhouse gases: A source-to-sea study of the River Clyde

Alison M. Brown [a,b,*], Adrian M. Bass [b], Ute Skiba [a], John M. MacDonald [b], Amy E. Pickard [a]

[a] UK Centre for Ecology & Hydrology (Edinburgh), Bush Estate, Penicuik, Midlothian, EH26 0QB, UK
[b] University of Glasgow, College of Science and Engineering, School of Geographical and Earth Sciences, University Avenue, Glasgow, G12 8QQ, UK

ARTICLE INFO

Keywords:
Methane
Nitrous oxide
Carbon dioxide
Urban wastewater
Agriculture
Mine water

ABSTRACT

There is growing global concern that greenhouse gas (GHG) emissions from water bodies are increasing because of interactions between nutrient levels and climate warming. This paper investigates key land-cover, seasonal and hydrological controls of GHGs by comparison of the semi-natural, agricultural and urban environments in a detailed source-to-sea study of the River Clyde, Scotland. Riverine GHG concentrations were consistently oversaturated with respect to the atmosphere. High riverine concentrations of methane (CH_4) were primarily associated with point source inflows from urban wastewater treatment, abandoned coal mines and lakes, with CH_4-C concentrations between 0.1 - 44 μg l^{-1}. Concentrations of carbon dioxide (CO_2) and nitrous oxide (N_2O) were mainly driven by nitrogen concentrations, dominated by diffuse agricultural inputs in the upper catchment and supplemented by point source inputs from urban wastewater in the lower urban catchment, with CO_2-C concentrations between 0.1 - 2.6 mg l^{-1} and N_2O-N concentrations between 0.3 - 3.4 μg l^{-1}. A significant and disproportionate increase in all GHGs occurred in the lower urban riverine environment in the summer, compared to the semi-natural environment, where GHG concentrations were higher in winter. This increase and change in GHG seasonal patterns points to anthropogenic impacts on microbial communities. The loss of total dissolved carbon, to the estuary is approximately 48.4 ± 3.6 Gg C yr^{-1}, with the annual inorganic carbon export approximately double that of organic carbon and four times that of CO_2, with CH_4 accounting for 0.03%, with the anthropogenic impact of disused coal mines accelerating DIC loss. The annual loss of total dissolved nitrogen to the estuary is approximately 4.03 ± 0.38 Gg N yr^{-1} of which N_2O represents 0.06%. This study improves our understanding of riverine GHG generation and dynamics which can contribute to our knowledge of their release to the atmosphere. It identifies where action could support reductions in aquatic GHG generation and emission.

1. Introductions

Greenhouse gas (GHG) evasion from inland waters is a significant source of atmospheric GHGs. Global carbon dioxide (CO_2) evasion has been estimated as 1.8 ± 0.25 Pg C yr^{-1} from streams and rivers, resulting in a global evasion rate from inland waters of 2.1 Pg C yr^{-1} (Raymond et al., 2013). The contribution from streams and rivers is large relative to their surface area, acting as hotspots for the exchange of gases with the atmosphere. The major sources of CO_2 are direct input via groundwater inflow, which transports CO_2 originating from soil respiration, and in-stream mineralization of organic carbon (OC) often from surface run-off (Winterdahl et al., 2016). Riparian wetlands also contribute disproportionately to CO_2 emissions (Abril and Borges, 2019). The relative importance of these mechanisms changes with stream order as headwater streams have a larger soil-water interface compared to lower reaches, resulting in the proportion of CO_2 produced from aquatic metabolism increasing with stream size (Marx et al., 2017; Hotchkiss et al., 2015). The magnitude of CO_2 riverine emissions is highly dependant on hydrology (Gómez-Gener et al., 2016). In urban areas significantly higher nutrients, organic matter content, and riverine cyanobacteria impact CO_2 variation (Salgado et al., 2022). Global methane (CH_4) evasion from inland waters was estimated at 398.1 ± 79.4 Tg CH_4 yr^{-1}, with rivers evading 30.5 ± 17.1 Tg CH_4 yr^{-1}, with aquatic ecosystems contributing about half of total global CH_4 emissions from anthropogenic and natural sources (Rosentreter et al., 2021). Total CH_4 emissions were found to increase from natural to impacted and from coastal to freshwater ecosystems, with emissions expected to increase due to urbanization, eutrophication and positive climate feedbacks,

* Corresponding author at: –UK Centre for Ecology & Hydrology.
E-mail address: albrown52@ceh.ac.uk (A.M. Brown).

https://doi.org/10.1016/j.watres.2023.119969
Received 11 December 2022; Received in revised form 1 April 2023; Accepted 9 April 2023
Available online 12 April 2023

although there is significant uncertainty in the production, transportation and consumption processes (Rosentreter et al., 2021, Stanley et al., 2016). Similarly the production and emission of nitrous oxide (N_2O) from aquatic systems are uncertain (0.3 – 2.1 Tg N_2O-N yr^{-1}) with large spatial and temporal variability in emission estimates (Seitzinger and Kroeze, 1998; Beaulieu et al., 2011; Ciais et al., 2013). However N_2O emissions from rivers, reservoirs and estuaries have been estimated as 148 – 277 Gg N yr^{-1} with anthropogenic perturbations to river systems resulting in a two to four-fold increase in N_2O emissions from inland waters (Maavara et al., 2019). The dominance of N_2O emissions emanating from nitrification or denitrification in inland waters is partly dependant on residence time (Zarnetske et al., 2011).

Urban rivers and lakes are potential hotspots for GHG emissions and there is an increasing body of literature concerned with quantifying their contribution to aquatic GHG emissions (Zhang et al., 2021; Wang et al., 2021; Gu et al., 2021; Herrero Ortega et al., 2019; Martinez-Cruz et al., 2017 and Garnier et al., 2009). In Mexico City water quality indicators (such as trophic state index and phosphorous level) were positively correlated with CH_4 emissions, suggesting a reduction in untreated wastewater discharge could concurrently reduce GHG emissions. Fluxes of CH_4 were highly variable, both in and across ecosystem locations and seasons (Martinez-Cruz et al., 2017) demonstrating the need for comprehensive studies to understand these temporal dynamics. In water bodies around the city of Berlin, a combination of high nutrient supply and shallow depth produced large CH_4 emissions. However dissolved oxygen and productivity were found to be poor predictors of CH_4 emissions, suggesting a complex combination of factors governed CH_4 fluxes from urban surface waters (Herrero Ortega et al., 2019). Conversely in rivers and lakes within the city of Beijing, high CH_4 emissions were attributed to high dissolved and sediment organic carbon, high aquatic primary production and shallow water depths, although results were again highly variable (Wang et al., 2021). In the Chaohu Lake basin in eastern China, diffusive CH_4 and N_2O emissions from rivers were due to large nutrient supply and hypoxic environments, with CO_2 impacted by temperature-dependant rapid decomposition of organic matter (Zhang et al., 2021). Positive correlations between temperature and GHG concentrations have been routinely observed (Wang et al., 2021; Herrero Ortega et al., 2019 and Rosentreter et al., 2021). The presence of ammonia, entering inland water from agriculture or wastewater, can inhibit CH_4 oxidation resulting in elevated CH_4 concentrations compared to low nitrogen systems and high evasion to atmosphere (Dunfield and Knowles, 1995; Bosse et al., 1993; Cotovicz et al., 2021). Conversely in an investigation of N_2O concentrations upstream and downstream of wastewater treatment plants (WWTPs) in an urban river in Japan, lower N_2O concentrations were found in summer (Y. Zhou et al., 2022). Positive correlations between GHGs in surface waters and catchment agricultural landcover linked to higher levels of organic matter and dissolved inorganic nitrogen from the agricultural dominated areas have been found significant, with increases in GHG levels during prolonged low water levels (Borges et al., 2018).

GHG emissions are difficult to attribute to sources due to multiple generation and consumption pathways and high spatial and temporal variability (Rosentreter et al., 2021). Their production results from the interplay of multiple drivers and is influenced by, high between and within-system variation, with the causes of this variation unknown. This variation causes difficulties in upscaling emissions from local-scale studies resulting in a need for more detailed studies measuring more in-water parameters across a large temporal and spatial scales. It is hypothesised, in this paper, the reasons for the high variation and poor predictably include:

1 GHGs are not conserved like dissolved nutrients but readily out-gas especially in the riverine environment with flow intensity and high stream slopes the primary controls (Long et al., 2015;Maurice et al., 2017; Natchimuthu et al., 2017; Liu and Raymond, 2018).
2 The number of different source types within the riverine environment, including: point, diffuse and in-water generation, change with land-use and need to be distinguished.
3 The concentration of nutrients is only one aspect of GHG generation, which changes with availability of electron donors and acceptors, such that mixing of waters may stimulate GHG production (Wrage et al., 2001; Furukawa et al., 2004; Broder et al., 2012; Zhang et al., 2019).
4 Different GHG sources and dynamics dominate in different types and sizes of water body dependant on: land-water interface, depth, hydraulic regime, sediments-water-air interfaces, residence time, land-use, physio-chemical properties, microbial communities, seasonality, and anthropogenic impacts on seasonal patterns of changing water level and temperature.

The concentrations of GHGs in the riverine water column result from the balance between input, consumption, production and output (Fig. 1).

Given the potential significance, but inadequate quantification and characterisation of urban catchment fluvial GHG dynamics, further insight into how to quantify and interpret riverine GHG concentration data could support improved estimates. This study addressed the following key objectives: (1) does using a source-to-sea investigative approach allows quantification of how changes in the nature and size of the riverine environment impact GHG concentrations, (2) can the key controls on GHG generation be determined by comparison of the semi-natural, agricultural and urban environments, including key land-cover, seasonal and hydrological controls, and (3) can point source, diffuse source and in water generation be distinguish for different GHGs. A large temperate catchment was selected for the investigation, where landcover transitioned from semi-natural, through pastoral and arable agricultural to urban (including legacy industrial), as representative of many urbanised catchments globally.

2. Materials and method

2.1. Study area

The River Clyde is the third longest river in Scotland (170 km) with a total river network length of 4244 km and drains a of 1903 km^2 (Clyde River Foundation, 2020). The River Clyde together with the rivers Kelvin, White Cart, Black Cart and Leven enter the Clyde estuary, with a catchment area of 3854 km^2 (Nedwell et al., 2002), which is home to 33.8% (1.79 million) of Scotland's total population (Clyde River Foundation, 2020). Surface water quality, as assessed in accordance with the European water framework directive (SEPA, 2018 and Natural Scotland, 2015), ranges from 'High' in some small tributaries to 'Bad' in some urban tributaries, with much of the River Clyde rated as 'Moderate'. The groundwater quality is also rated as 'Poor', both in the upper catchment in the Leadhills area and the lower urban catchment. The River Clyde's mean annual flows is 48.3 $m^3 s^{-1}$ with the maximum flow of 560.5 $m^3 s^{-1}$ (24th January 2018) as measured at Daldowie gauging station (supplementary data Table A1.1) based on data between 1963 and 2019 (UK Centre of Ecology & Hydrology (UKCEH), 2020). The upper moorland catchment consists of steep rough ground with hill pasture and some forestry as the major land use. In the middle catchment there is mixed farming including arable and pastoral and significant urbanisation in the lower catchment.

2.2. Sites description and data collections

Twenty-six measurement locations were selected on the River Clyde and its major tributaries. The locations were distributed along the River Clyde from near the source on Daer Water, above Daer reservoir, to Glasgow Green just above the Clyde tidal weir, which separates two distinct habitats of fresh and salt water. The sample locations are shown

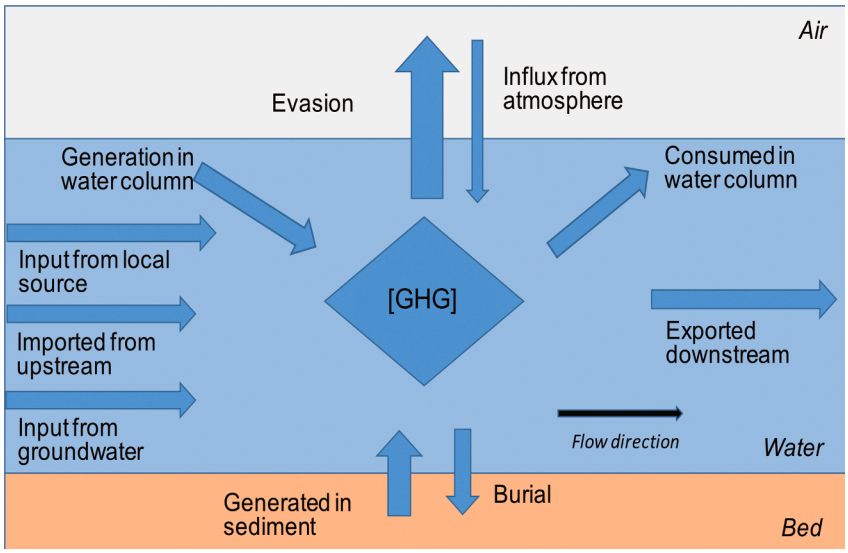

Fig. 1. GHG generation, transport and loss. In the schematic the arrows show the direction of GHG movement into/out-from the sediment (brown), water (blue) and air (grey). The balance between the different sources and sinks changes along the river course. Both river slope and hydrology impact this balance as they influence water residence times, sedimentation, out-gassing and nutrient concentrations from point and diffuse sources. (For interpretation of the references to colour in this figure legend, the reader is referred to the web version of this article.)

spatially against both the water network of the River Clyde and tributaries (Fig. 2A) and the catchment land cover (Fig. 2B). Full details of the survey locations are provided in the supplementary information Table A1.1 with photographs in Figure A2. Samples were collected monthly between January 2020 and December 2021 at all locations. Twenty-one sampling campaigns were undertaken as no sampling was permitted during the period April to June 2020 due to Covid-19 working restrictions. Each sampling campaign was undertaken over two consecutive days with samples collected at the upper catchment sites on day one and in the lower catchment on day two. Sample filtration and processing was undertaken on the same day as sample collection.

2.3. Field sampling and laboratory measurements

Dissolved gas samples were collected in triplicate at each location using the headspace method, prior to the collected water being

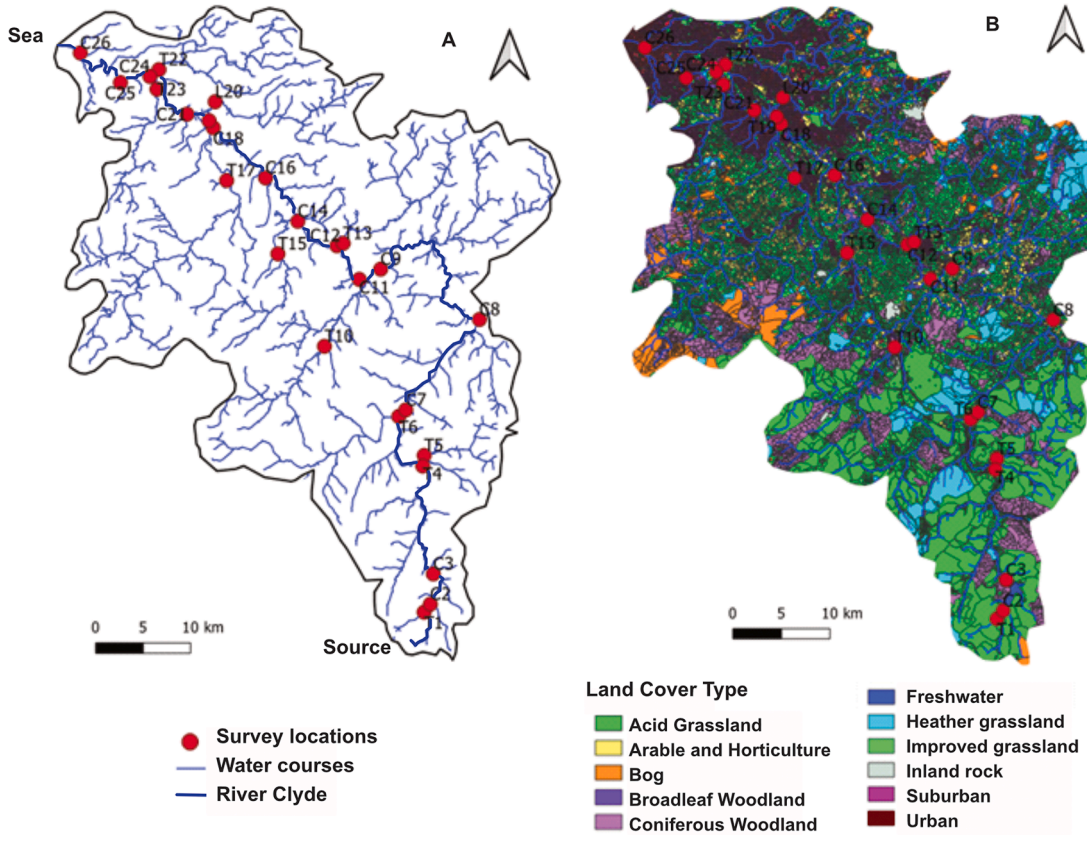

Fig. 2. Spatial plots of the River Clyde catchment. Panel A shows the River Clyde and tributaries (Ordnance Survey, 2022) and Panel B shows the land cover (UK Centre for Ecology & Hydrology (UKCEH), 2020). The source-to-sea survey locations are denoted with the lowest number near the source of the River Clyde and the highest number near the river-sea interface. The measurements on the River Clyde are indicated by a `C` and the tributaries by a `T` and where the tributary is direct inflow from a loch this is indicated by an `L`.

disturbed by other measurements, together with ambient air samples (Billett and Moore, 2008). Conductivity (EC), water temperature (T_W), dissolved oxygen concentration (DO) and pH were measured, and a two-litre water sample was retained for later analysis, which was kept in a dark, cool-box until returned to the laboratory for processing, to minimise biological activity. Full details of the data collection and laboratory measurement methodologies are described (Brown et al., 2023).

Headspace samples were analysed using an Agilent 7890B gas chromatograph (GC) and 7697A headspace auto-sampler (Agilent, Santa Clara, California), with CO_2, CH_4 and N_2O concentrations determined by running gas vials containing four mixed gas standards prepared in a consistent way to the ambient air samples. The concentrations of the standards gases were: 1.12 to 98.2 ppm for CH_4; 202 to 5253 ppm for CO_2; and 0.208 to 1.04 ppm for N_2O. Water samples were filtered within 12-hrs of collection through a Whatman GF/F 0.7 μm, under vacuum. Filtrate was then analysed for: total dissolved nitrogen (TDN), total dissolved carbon (TDC) and dissolved organic carbon (DOC), anion & cation concentration, UV–Vis absorbence. Total phosphorus (TP) analysis was undertaken on unfiltered samples. Analysis for TDN, TDC and DOC were undertaken using a Shimadzu TOC-L series Total Organic Carbon Analyser with all samples run within 36-hrs of collection. The difference between TDC and DOC was used to calculate dissolved inorganic carbon (DIC). The filtration resulted in outgassing of gases including CO_2 raising the pH, such that most DIC measured by this method was in the form of bicarbonate and will underestimate the total DIC in the original stream waters (bicarbonate plus CO_2). Absorbence at 254 nm, indicative of aromaticity, was measured using a Perkin Elmer LAMBDA® 365 UV–Vis Spectrophotometer to evaluate the Specific Ultraviolet absorbence (SUVA). A low $SUVA_{254}$ indicates a smaller portion of aromatic humic matter present in the water and can be used as an indicator of the anthropogenic impact (Williams et al., 2016). Ion chromatography using a Metrohm 930 Compact IC Flex was undertaken to determine both anion and cation concentrations. A mixed ion standard containing 11,000 ppm chloride (Cl^-), 5000 ppm nitrate (NO_3^-), 4000 ppm sulphate (SO_4^{2-}), 10,000 ppm sodium (Na^+), 5000 ppm ammonium (NH_4^+), 1000 ppm potassium (K^+), 1000 ppm calcium (Ca^{2+}) and 1000 ppm magnesium (Mg^{2+}), was diluted to make 7 standard solutions for calibration. These included dilutions of 0.1:100, 0.5:100, 1:100, 2:100, 5:100, 10:100, and 25:100. Total phosphorous (TP) was measured using a SEAL AQ2 analyser. Four standards were included in each run for calibration of between 0.025 to 0.20 mg P L^{-1}. Where concentrations exceeded the top standard, the machine diluted and re-measured the sample. For all techniques all sample points from each survey were run together.

2.4. Gas partial pressures

To calculate dissolved gas concentrations and partial pressures from the headspace equilibration method the following mass-balance equation was applied (Hamilton, 2006).

$$\left(C_{0liq}\right).\left(V_{ila}\right) + \left(C_{0gas}\right).\left(V_{gas}\right) = \left(C_{liq}\right).\left(V_{liq}\right) + \left(C_{gas}\right).\left(V_{gas}\right) \quad (1)$$

Where: C_{0liq} and C_{0gas} are the original gas concentration, C_{liq} and C_{gas} are the concentrations in the liquid and gas phases after equilibration (shaking) and V_{liq} and V_{gas} are the volumes of the liquid and gas in the syringe (assumed to be the same before and after shaking). Assuming equilibrium inside the vessel then C_{liq} can be replace by:

$$C_{liq} = P_{gas}.\beta_T.P_{BAR} \quad (2)$$

Where: P_{BAR} is the barometric pressure at the measurement time and altitude, P_{gas} is the partial pressure in the gas phase, β_T is the Bunsen solubility coefficient as a function of temperature. This can be rearranged:

$$\left(C_{0liq}\right) = \left(P_{gas}.\beta_T.P_{BAR}\right) + \left(C_{gas} - C_{0gas}\right).\left(V_{gas}\right)/\left(V_{liq}\right) \quad (3)$$

This gas concentration in μmoles/L can be converted to units of ppmv using the Ideal Gas Law, where ppmv = (μmoles/L).(RT), where R is the gas constant and T is the temperature in Kelvin.

This method is effective for CH_4 and N_2O but can lead to errors in CO_2 estimates as dissolved CO_2 is in dynamic chemical equilibrium with other carbonate species. The error incurred by headspace analysis of CO_2 is less than 5% for typical samples from boreal systems which have low alkalinity (<900 μmolL^{-1}), with pH <7.5, and high pCO_2 (>1000 μatm). This was the case for (98% of the samples here but errors in the lower Clyde tributaries, with both higher alkalinity and pH, were estimated as reaching 10% (Koschorreck et al., 2021).

2.5. Data sources and processing

Flow data measured by SEPA at their various gauging stations was used for all hydraulic calculations, details of the data applied at each location are provided in the supplementary information Table A1.1 (Scottish Environment Protection Agency, 2020 and (UK Centre of Ecology & Hydrology (UKCEH), 2020). River flow, over the period January 2020 to December 2021, for the Sills of Clyde in the upper catchment ranged between 2.5 and 345 m^3 s^{-1} (the survey captured a range of 3.3 - 113 m^3 s^{-1}) and Daldowie in the lower catchment ranged between 4.8 and 522 m^3s^{-1} (the survey captured a range of 5.6 - 170 m^3 s^{-1}) (Fig. 3A & B). The River Clyde experiences significant height loss between 75 and 100 km from source, which would be expected to produce significant outgassing (Fig. 3C), and significant inputs from urban wastewater treatment (UWWT) and mine water outflows (MW) (Fig. 3D).

Data was analysed using a combination of approaches. Spatial analysis of all measured parameters was undertaken using Quantum Geographic Information System (QGIS) version 3.22. Land cover analysis was undertaken by generation of the catchment area for each measurement point and applications of a land cover date; (UK Centre for Ecology & Hydrology (UKCEH), 2020) also using QGIS. Pearson's correlation was applied to determine relationships between the GHG concentrations, water physiochemical properties and land cover. Locations were grouped using K-cluster analysis, to help investigate the impact of seasonality, based on measured water chemical properties (DOC, DIC, TDN, TP, Cl^-, NO_3^-, SO_4^{2-}, Na^+, NH_4^+, K^+, Ca^{2+} and Mg^{2+}). Physical parameters such as temperature (which mainly distinguish sites by elevation) and conductivity (a function of all dissolved ions) were not included.

Load appointment modelling (Bowes et al., 2008) was applied to all the GHG and chemical concentration data at all locations where flow data was available or could be calculated. The difference in the occurrence of point and diffuse sources is linked to the concentration-flow relationship, and can be calculated by using Eq. (4), where Q is volumetric flow rate and C_P and C_D are the point and diffuse source concentrations respectively. The constants A, B, C and D need to be calculated by iteration for each solute (Bowes et al., 2008). The models for the point and diffuse sources once generated were then applied to the full 2 years of flow data from January 2020 to December 2021 to determine volume transport for each GHG or solute.

$$C_T = C_P + C_D, \text{ where } C_P = A.Q^{(B-1)} \text{ and } C_D = C.Q^{(D-1)} \quad (4)$$

3. Results

3.1. GHG concentrations and water contamination from source-to-sea

Maximum concentrations for all GHGs occurred in the river urban section during July-September 2021, where concentrations reached; CH_4-C 44 μgL^{-1}, CO_2-C 2.6 mg L^{-1} and N_2O-N 3.4 μgL^{-1}, with corresponding saturations of 130,400%, 1170% and 1310%, respectively. All GHG concentrations exhibited both strong spatial and temporal variability. Riverine dissolved GHGs (CH_4, CO_2 and N_2O) were typically

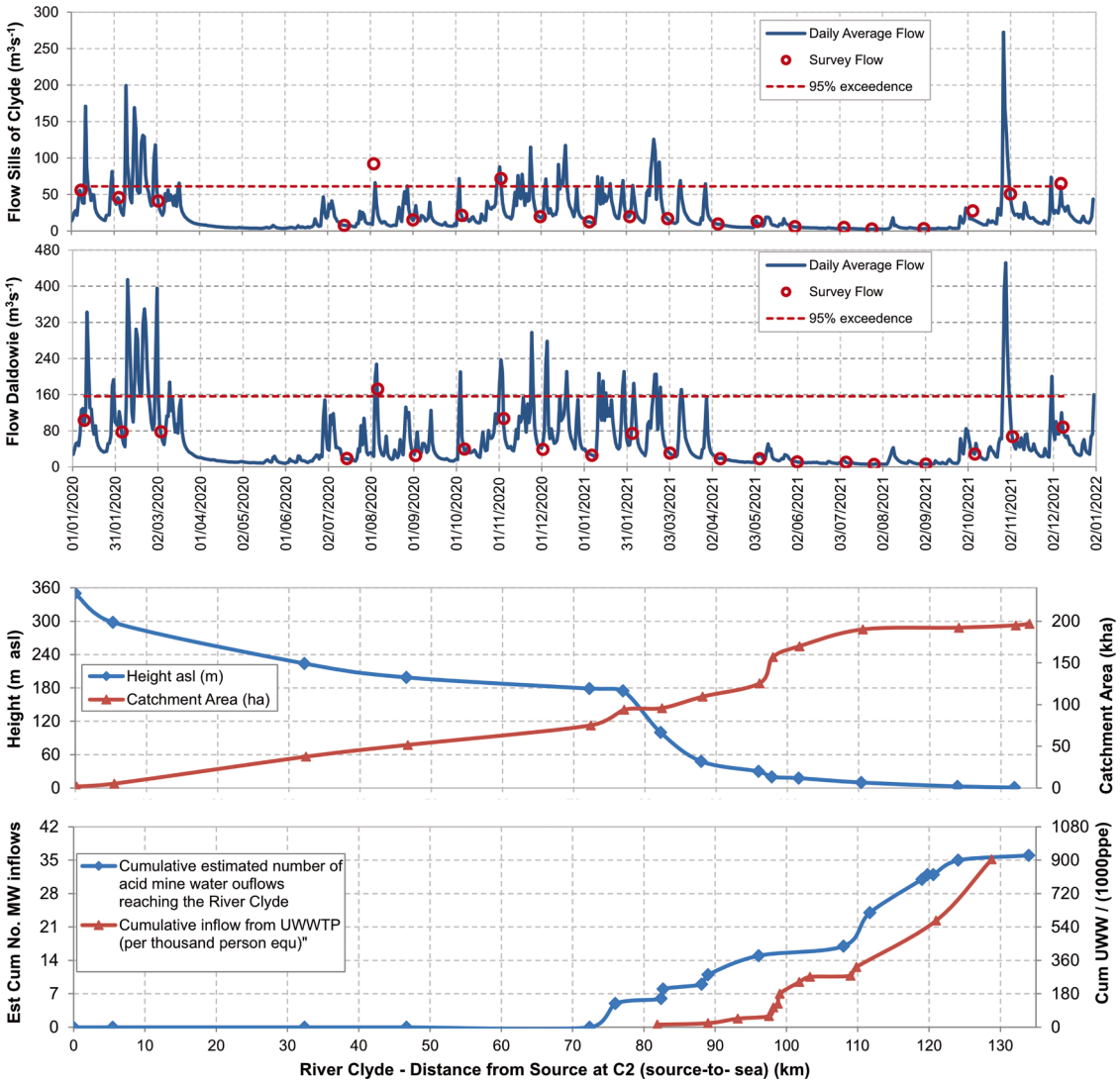

Fig. 3. River Clyde volumetric flow and contaminant inputs, The first two panels show the volumetric flow (Q) for the upper (Sills of Clyde) (A) and lower (Daldowie) (B) River Clyde relative to the survey dates for the first and second days of the surveys respectively. Effort was made to get consistent riverine flows over the two days of sampling, although during high river flows this was not possible (e.g. August 2020). In the spring and summer of 2021 (from April to September inclusive) a period of very low rainfall persisted, which was twice the duration as for 2020 and resulted in very dry conditions across the Clyde catchment. The third panel (C) shows the height and area of the Clyde catchment compared to distance from source for the different measurement points. The final panel (D) provides information on cumulative point sources entering the River Clyde from both urban wastewater treatment plants (UWWTP) in per 1000 person equivalent (1000ppe) and the cumulative number of known sources for Mine Water (MW) outflows. Note that this provides no information on the volume of MW entering the River Clyde or the degree of treatment. MW volumetric flow varies widely from different sources.

supersaturated with respect to the atmosphere, with >97% above the theoretical equilibrium value. The lowest saturations occurred in areas of steep slope and high turbulence, which included the head waters of the Clyde (C3) and the areas surrounding the Falls of Clyde (C12, T13, C14, T15, C16 and T17), with CH_4 showing the largest change in concentrations.

Riverine dissolved GHG (CH_4-C, CO_2-C and N_2O-N) and water physiochemical property (TP, TDN, DOC, DIC, Cl^-, NO_3^-, SO_4^{2-}, Na^+, NH_4^+, K^+, $Ca^{2+}$and Mg^{2+}) concentrations for the different locations measured on the River Clyde (Fig. 4A) and its tributaries (Fig. 4B) all increased from source-to-sea, in line with increasing percentage of both agricultural and urban land cover (Fig. 4C). Average concentrations for all locations are included in supplementary data Tables A3.1 and A3.2.

3.2. Land cover relationship with and methane and nitrous oxide dynamics

To determine land cover influences on nutrient and GHG concentrations, the land cover was correlated to the measured GHG concentrations and water physio-chemical properties (Table 1 and supplementary data Table A4.1). Analysis was for the tributaries and Clyde headwaters only, to ensure all data was independent and points within the analysis were on a similar spatial scale (catchment area < 250km^2). The measurements points in the lower urban River Clyde catchments (with the highest GHG concentrations) are not included to avoid confounding of data.

Conductivity, pH, TDN, TP, DIC, DOC, Cl^-, NO_3^-, SO_4^{2-}, Na^+, NH_4^+, K^+, Ca^{2+}, $Mg^{2+}$and N_2O-N were strongly negatively correlated with percentage cover of acid (semi-natural) grassland and positively correlated with improved (pasture) grassland, suggesting that acid grassland behaved as a nutrient sink while improved grassland behaved as a

Fig. 4. Radar plots of average dissolved GHGs and water chemical properties, The top panels are radar plots of average dissolved GHGs (CH_4-C, CO_2-C and N_2O-N) and water chemical properties (TP, TDN, DOC, DIC, Cl^-, NO_3^-, SO_4^{2-}, Na^+, NH_4^+, K^+, $Ca^{2+}$and Mg^{2+}). The source-to-sea survey locations are denoted with numbers from 1 (source) to 26 (sea), with the River Clyde indicated by a `C` and the tributaries by a `T` or `L`, where direct inflow is from a loch. The top left panel (A) is a source-to-sea progression of the River Clyde (coloured brown-green-blue) clearly demonstrating how the concentrations increase downstream. All data are normalised to the maximum average value for any survey location. The top right panel (B) is a source-to-sea progression for the Clyde tributaries, with tributaries joining in the upper Clyde (green), the middle Clyde (red-orange) and the lower Clyde (blue) and exhibiting a similar progression of concentrations. All data are normalised to the maximum average value for any survey location. The lower panel (C) shows the percentage land cover change between each location from source-to-sea on the River Clyde for comparison with panel A. Semi-natural (acid grassland, heather and forest) is in green, agricultural (arable and improved grassland) in light blue and urban (urban and suburban) in dark blue (UK Centre for Ecology & Hydrology, 2020). (For interpretation of the references to colour in this figure legend, the reader is referred to the web version of this article.)

Table 1
Pearson's Correlation Coefficient between nutrients and GHGs (EC, DO%, pH $SUVA_{254}$, TP, DOC, DIC, TDN, CH_4, N_2O and CO_2) and percentage land-cover across all Clyde tributaries and headwaters.

	CH_4	CO_2	N_2O	EC	DO%	pH	DOC	DIC	TDN	TP	$SUVA_{254}$
Acid grassland	−0.38	0.06	−0.40	**−0.84**	0.24	**−0.84**	**−0.88**	**−0.77**	**−0.94**	**−0.93**	**0.79**
Arable & horticulture	**0.51**	−0.05	0.07	**0.65**	−0.06	**0.73**	0.48	**0.77**	**0.74**	**0.67**	−0.63
Bog	0.04	−0.41	0.02	0.36	0.23	0.63	**0.64**	0.27	0.61	**0.77**	−0.41
Coniferous woodland	0.05	0.28	0.08	0.16	0.15	0.05	0.61	0.20	0.27	0.30	−0.11
Freshwater	0.12	−0.05	−0.10	−0.10	0.13	−0.03	−0.22	−0.09	−0.10	−0.16	−0.04
Heather	−0.15	−0.20	−0.01	0.19	−0.01	0.08	0.55	0.08	0.33	0.14	−0.27
Heather grassland	−0.03	0.13	0.15	−0.05	−0.21	−0.22	0.10	−0.06	−0.10	−0.07	−0.06
Improved grassland	0.21	−0.20	0.38	**0.76**	−0.18	**0.82**	**0.91**	**0.64**	**0.91**	**0.94**	**−0.70**
Inland rock	**0.71**	**0.56**	0.55	**0.73**	−0.55	0.48	0.36	**0.85**	0.54	0.44	−0.51
Urban & Suburban	**0.59**	**0.06**	0.49	**0.88**	**−0.56**	**0.85**	0.36	**0.84**	**0.78**	**0.70**	**−0.81**

Notes
[1]Values are the Pearson's correlations coefficient with the values in bold considered significant with at P-value < 0.05.
[2]There is a strong correlation between broadleaf woodland and urban and suburban land-cover within the Clyde catchment (R^2 =0.91, P-value <0.001), possibly because broadleaf woodland has been planted within the suburban and urban environment. Hence broadleaf woodland has not been included.
[3]To ensure all data points are independent only tributaries and the upper River Clyde are included. As a result the lower Clyde points (including the large UWWTP linked to high CH_4 concentrations) are not included to avoid confounding of catchments.

nutrient source. Arable & horticulture (arable) cover was positively correlated with EC, pH, DIC, TDN, TP, Cl^-, NO_3^-, NH_4^+, K^+, Ca^{2+}, $Mg^{2+}$and behaved as a nutrient source. The area of arable & horticulture cover is an order of magnitude lower than for improve grassland, but correlations are similar (Table 1 and supplementary data Table A4.1).

Urban & suburban (urban) cover was strongly positively correlated with EC, pH, TDN, TP, DIC, Cl^-, NO_3^-, SO_4^{2-}, Na^+, NH_4^+, K^+, Ca^{2+}, Mg^{2+}, CH_4-C and N_2O-N suggesting that the urban cover acts as both a nutrient and GHG source. Urban land cover was negatively correlated with DO% while other land-cover types had no statistically significant impact of river oxygenation. Improved grassland, urban and arable cover were all negatively correlated with $SUVA_{254}$ suggesting an anthropogenic

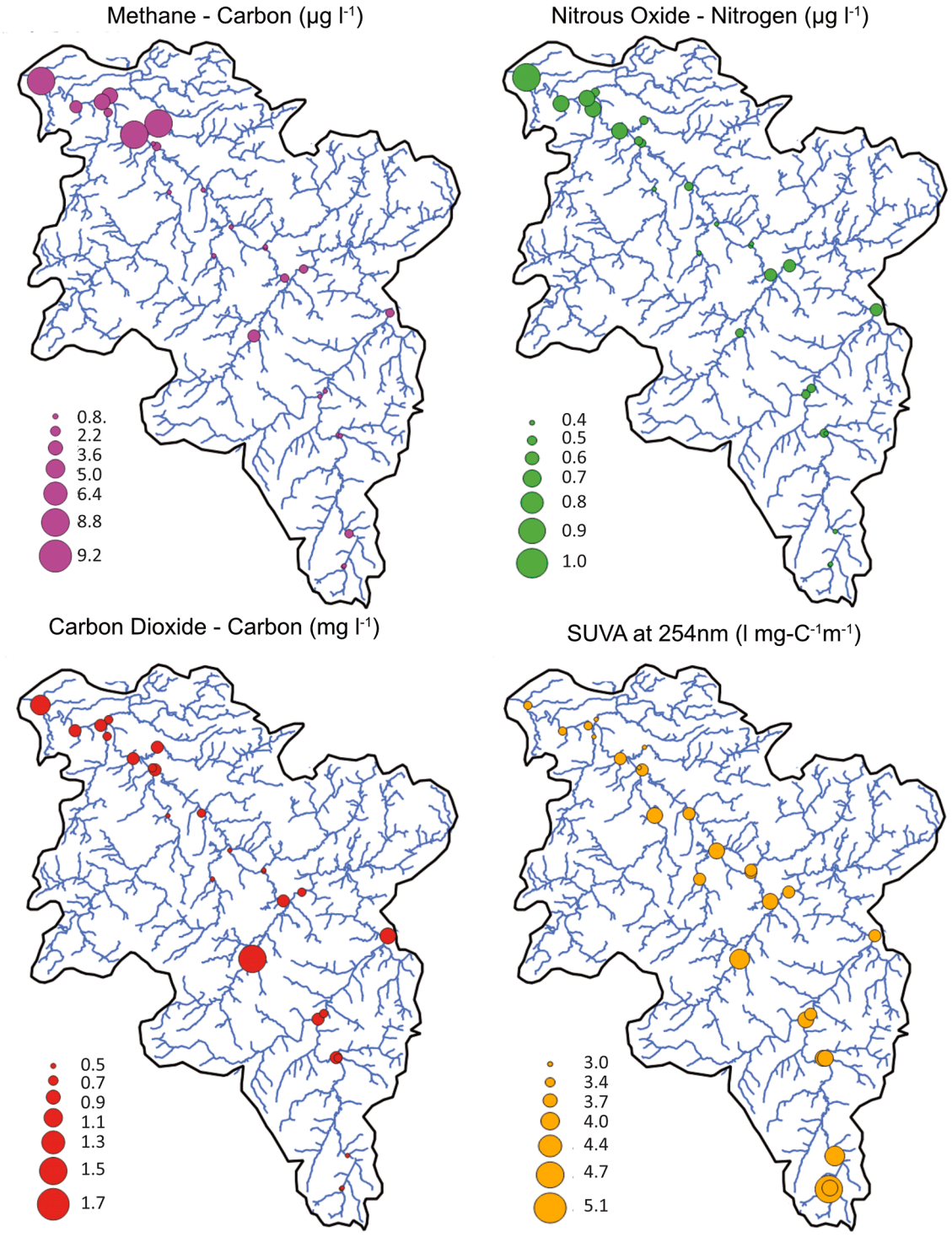

Fig. 5. Spatial average of CH_4, CO_2, N_2O and SUVA at 254 nm **across the Clyde catchment.** The average concentration data for CH_4-C, N_2O-N, CO_2-C and $SUVA_{254}$ shown spatially (for T_W, EC, pH, DO, TP, TDN, DOC, DIC, Cl^-, NO_3^-, SO_4^{2-}, Na^+, NH_4^+, K^+, Ca^{2+}, Mg^{2+}see supplementary information Figure A5). The size of the marker denoting the average concentration / value at each measured location. The concentrations of all three GHGs (CH_4-C, CO_2-C and N_2O-N) are low in the middle Clyde catchment due to high out-gassing corresponding to regions of high turbulence. Both CH_4 and N_2O concentrations are high in the lower catchment. Both CH_4-C and CO_2-C concentrations are elevated in tributaries that have significant MW inflow (e.g., at T10). The $SUVA_{254}$ values decrease from the upper to lower catchment.

influence as land cover linked to nutrient concentrations and human density have been found to impact humic composition (Williams et al., 2016). No statistically significant correlations are detected for CO_2 (Table 1 and supplementary data Table A4.2).

3.3. GHG spatial heterogeneity

The spatial patterns of CH_4, N_2O and CO_2 are similar, with the lower (urban) catchment to the northwest having the highest concentrations (Fig. 5). The concentrations of CH_4, N_2O and CO_2 in the middle catchment associated with the Falls of Clyde (C12-C18, 78 to 100 km from source), an area of high turbulence with an elevation drop of 150 m, were the lowest and are typically at or near atmospheric equilibrium, likely associated with high evasion due to increased turbulence. The upper more rural catchment has more variability between the different GHGs. For example, T10 has both high CH_4 and CO_2 but lower relative N_2O concentrations and was observed associated with MW inflows, conversely the C9 has higher N_2O but lower relative CH_4 and CO_2 concentrations and has high agriculture land cover.

Average $SUVA_{254}$ values of 5 (35% aromaticity) occured in the upper catchment dropping to 3 (20% aromaticity) in the lower catchment. The three most urban tributaries (T19, T22 & T23) consistently demonstrated the lowest $SUVA_{254}$ values, characteristic of high anthropogenic impact. The spatial patterns for DIC, SO_4^{2-}, Ca^{2+}, Mg^{2+} and K^+ (supplementary data Figure A5) are similar and exhibit high concentrations in the tributary measurements (T10, T13, T19, T22), all of these catchments are influenced by legacy coal mines and outflows of MW (Fig. 3D). The tributary T23 also exhibited high SO_4^{2-} and Na^+ compared to other ions suggestive of a different industrial legacy waste history. The Ions, Cl^-, NO_3, $Na^+$and NH_4^+, all increase with urbanisation of the catchment and are consistent with anthropogenic sources (Herlihy et al., 1998).

Table 2
Cluster analyses based on the measured water chemical properties (DOC, DIC, TDN, TP, Cl^-, NO_3^-, SO_4^{2-}, Na^+, NH_4^+, K^+, Ca^{2+} and Mg^{2+}) distinguishes locations by position in the catchment.

No	Cluster Name	Locations	Description
1	Upper Clyde-Agricultural	**C7, C8, C9**	Upper section of the River Clyde, with both pastoral and arable agriculture
2	Middle Clyde-suburban arable	**C11, C12, C14, C16, C18**	Middle section of the River Clyde with a mixed signal of suburban, mining and agriculture
3	Lower Clyde-highly urban	**C21, C24, C25, C26**	Lower section of the River Clyde, dominated by high urban land coverage and increases in Cl^-, TDN and TP
4	Upper tributaries-Semi-natural	**T1, C2, T4, T5, T6**	Upper Clyde tributaries, flowing from semi-natural or pastoral environments including streams from reservoirs.
5	Middle tributaries-rural plus mining	**T10, T14, T15, T17**	Middle Clyde tributaries, dominated by pastoral and arable agriculture, disused coal mines and DOC from peat
6	Lower tributaries-urban plus mining	**T19, T22, T23**	Lower Clyde tributaries, dominated by urban, coal mining and legacy industry with the highest concentrations of all ions.

Note:
[1]K-Cluster analyses based for 6 clusters using measured water chemical properties effectively distinguishes locations on the river Clyde and tributaries by their position in the catchment.
[2]C3 (measured below Daer reservoir) and L20 (Strathclyde Loch) were not included in the cluster analysis as these primarily represent lake properties rather than riverine properties.

3.4. Seasonal GHG distribution by land use characteristics

Locations were grouped using K-cluster analysis based on measured water chemical properties. The result with six clusters was selected and summarised in Table 2.

Seasonal patterns for riverine dissolved GHGs (CH_4, CO_2 and N_2O) and water physiochemical properties (TDN and TP) were investigated using the clustering in Table 2 and were found to be inconsistent throughout the catchment (Fig. 6). In the upper and middle catchment for both the River Clyde and its tributaries, CH_4 and TP concentrations exhibited low variability by season. However, in the lower urban catchments both the highest mean and maximum concentrations occured in summer and autumn. Concentrations of CH_4 in the lower urban catchment increased by an order of magnitude and TP by at least four times. Conversely N_2O, CO_2 and TDN exhibited their lowest average values in summer with the highest values in spring and winter in the upper and middle catchments. However, in the lower urban catchment the seasonality pattern changes with the highest concentrations of N_2O, CO_2 and TDN in the summer.

The seasonal change in summer could be driven by temperature or reduced river flow. Temperature is correlated with reduced river flow and this correlation becomes more significant in the lower urban catchment (at C9 (upper catchment); $R^2 = 0.5$, p-value <0.03 and at C24 (lower catchment); $R^2 = 0.61$, p-value <0.003 (August 20 data excluded and log-linear relationship applied)). The low river flow in summer would impact contaminant and nutrient concentrations particularly where these are linked to point rather than diffuse sources. Thus this seasonal impact could be driven by temperature and concentrations of nutrients from point sources.

3.5. GHG, nutrient and contaminant correlations

Correlations over the whole catchment show that both CH_4 and N_2O were significantly positively correlated with TP, TDN, NO_3^- and NH_4^+ with CH_4 also significantly positively correlated with DIC and Mg^{2+} and N_2O significantly positively correlated with Cl^-, CH_4, CO_2 and N_2O are all negatively correlated with DO% (Table 3 and supplementary data Table A4.2). In the urban sector (L20 to C26) DO values are lower (supplementary data Table A3.1), suggesting reduced water aeration. Conductivity, DIC, Cl^-, SO_4^{2-}, Na^+, K^+, Ca^{2+}, Mg^{2+}, are all strongly inter-correlated. TDN is strongly correlated with NO_3^- but also TP. These correlations are not consistent across the whole the catchment and are investigated using the clustering from Table 2. The correlations for clusters 1, 3, 4 and 6 are shown in Fig. 7.

There are few significant correlations for GHGs in the upper catchment, especially for CH_4, N_2O is positively correlated with T_w, NO_3^+ and TDN, and CO_2 negatively correlated with DO% (Fig. 7A and B). However, in the lower urban catchment strong correlations occured between almost all GHGs and physiochemical properties, suggesting high GHG concentrations occured as contaminate concentrations increased and DO% decreased (Fig. 7C and D). The correlation between TDN and TP is high in the urban environment ($R^2 = 0.76$), both linked to UWW. This may result in some correlations which are unlikely to be causal. In the urban area CH_4 is highly correlated with TP and N_2O with TDN (associated with UWW), and CH_4 with the DIC, SO_4^{2-}, Ca^{2+} and Mg^{2+} grouping (associated with MW), suggesting different mechanisms for CH_4 production compared to the semi-natural environment. In the urban area significant negative correlations occured between both DO% and $SUVA_{254}$, and most physiochemical properties and GHG concentrations.

3.6. Drivers for greenhouse gas concentrations

A load apportionment model was used to model the GHG and solute concentrations and the exponents (B and D) from the relationships for concentration as a function of flow (Eq. (4)) were estimated for point and diffuse sources and used to distinguish four source types: (1) point

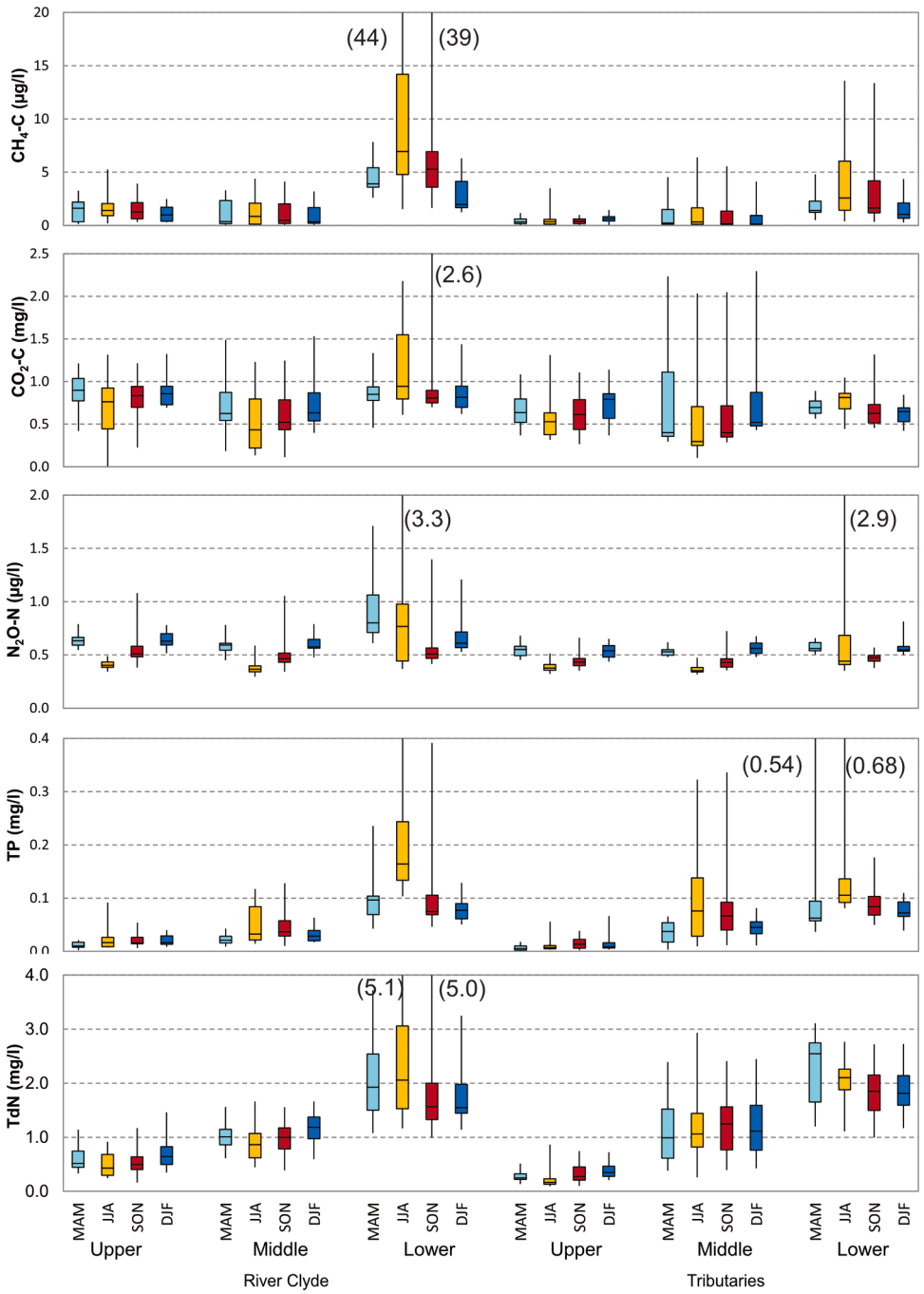

Fig. 6. Seasonal analysis of GHGs for the upper, middle and lower River Clyde and tributaries, Box plots of concentrations of dissolved CH_4-C, CO_2-C, N_2O-N, TDN and TP in the Clyde catchment, showing the median, 25% and 75% quantiles, minimum and maximum for a seasonal analysis: spring (March-May) in light blue, summer (June to August) in yellow, autumn (September to November) in red and winter (December to February) in blue. The results are grouped by six different regions of measurements on the upper, middle and lower River Clyde and tributaries that enter the River Clyde in the upper, middle and lower reaches. Seasonal trends that occur in the upper and middle catchment are changed when the Clyde enters the highly urban lower catchment. (For interpretation of the references to colour in this figure legend, the reader is referred to the web version of this article.)

Table 3
GHG correlation with water physiochemical properties over the whole Clyde catchment.

GHG	EC	T_W	pH	DO	DO%	DOC	DIC	TDN	TP	$SUVA_{254}$
CH_4-C	**0.41**	0.34	0.13	**−0.47**	**−0.42**	0.03	**0.41**	**0.43**	**0.45**	−0.18
CO_2-C	0.23	−0.04	−0.10	−0.28	**−0.64**	−0.02	0.19	0.23	0.19	0.02
N_2O-N	**0.49**	−0.14	0.12	−0.11	−0.38	0.01	0.16	**0.47**	**0.51**	−0.10

Notes:
(1) Additional GHG correlations with water physiochemical properties over the whole Clyde catchment are included in supplementary data - Table A4.2.
(2) Correlation significance increases when the catchment is divided between semi-natural, agrilcultural and urban.

sources which are fully independent of flow ($B = 0$), (2) point sources where concentration appears influenced by flow or rainfall ($0 < B < 1$), (3) diffuse sources where the concentration increases with flow ($D > 1$) and (4) diffuse sources where concentrations remain constant with flow ($D = 1$). The ions, nutrients and GHGs are categorised for these four source types in Table 4 and show different behaviours in the upper and lower catchment.

Mean concentrations together with calculated point and diffuse

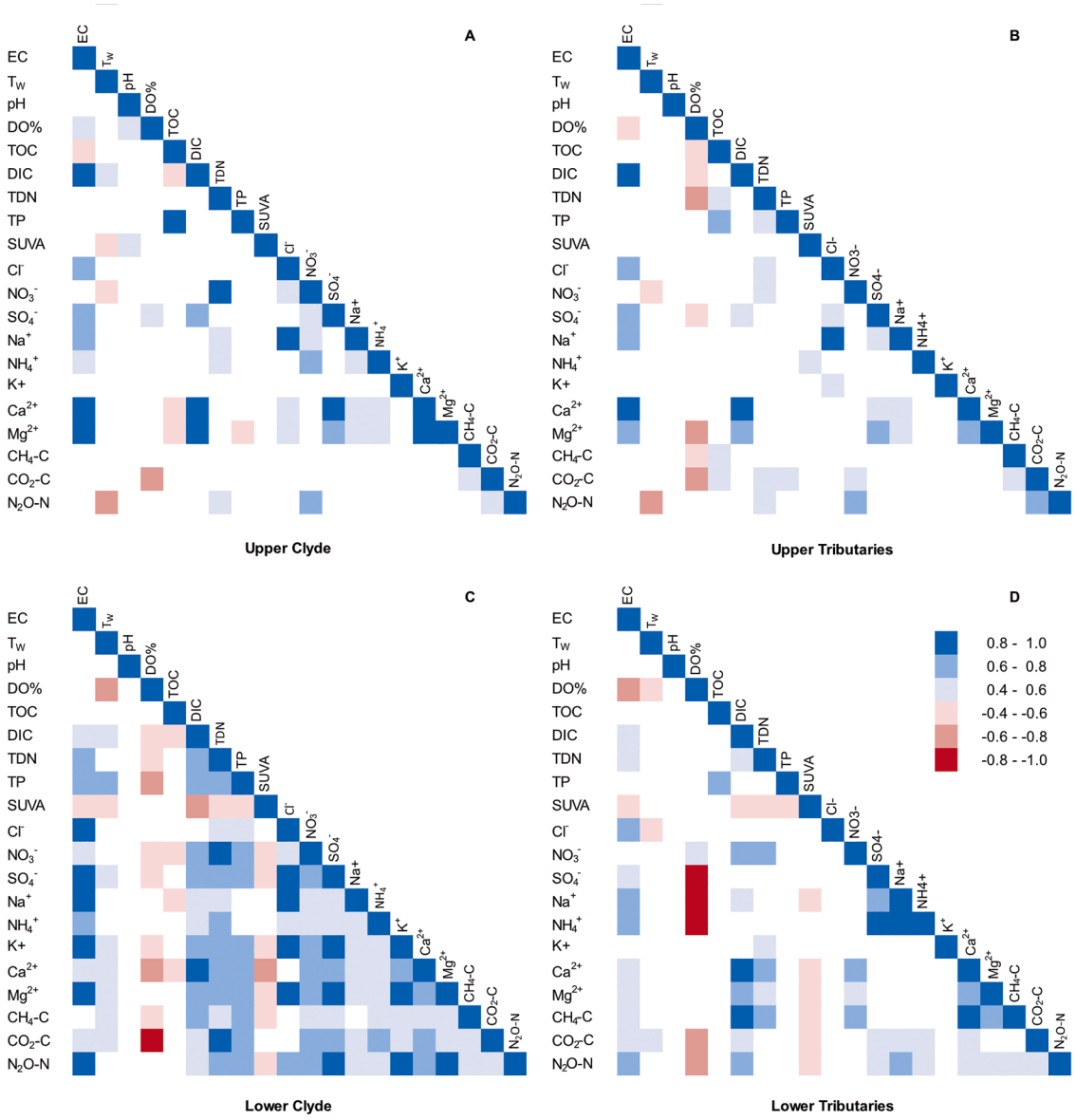

Fig. 7. Correlation between GHGs and physiochemical water properties, Correlations are for A) the upper and B) lower River Clyde and C) upper and D) lower Clyde tributaries as selected from the groups in Table 2. Positive correlations are depicted in blue and negative correlations in red with the stronger correlations in a darker shade. Positive correlations ⟨ 0.4 and negative correlations ⟩ −0.4 have been excluded as do not meet this significance criteria (p-value <0.005) Correlation increases in the lower catchment, with GHGs strongly correlated with contaminates and inversely correlated with DO%.

concentrations for the River Clyde from source-to-sea (Fig. 8 and supplementary data Figure A6), show the increasing significance of point source inputs in the lower urban river for both GHGs and nutrients. In the upper catchment GHG concentrations were dominated by diffuse agricultural sources. In the lower, urban catchment point sources became dominant over diffuse sources for CH_4, TP and $NH_4^+$and became significant for N_2O, CO_2, NO_3^- and TDN. Additionally, while NO_3^-, N_2O and CO_2 are dominated by diffuse flow their concentrations remain constant with flow, suggesting a reduced connection with their catchment. Generation of N_2O and CO_2 would be in the water column, with in-water generation and out-gassing approximately in balance (N_2O by (de)nitrification of dissolved nitrogen compounds and CO_2 by in-stream mineralization of DOC rather than input via groundwater). The CH_4 concentrations best reflect those of TP ($R^2 = 0.5$, P-value <0.005), while TDN concentrations are reflected in N_2O ($R^2 = 0.65$, P-value <0.0005) and CO_2 ($R^2 = 0.71$, P-value <0.0002) concentrations. The locations C21 (112 km from source) and C26 (134 km) (Fig. 8) show the highest concentrations of CH_4 and N_2O, which are within 0.3 km and 3.4 km of UWWTP outfalls. The tidal weir (400 m downstream of this C26) locally reduces flow and increases water residence times, which may act to reduce DO% seen at this location. The major point sources identified in the lower catchment included inflows from UWWTP and MW from abandoned coal mines (Fig. 3D).

3.7. Carbon and nitrogen exports to the estuary

Data measured at C26, was used to estimate the carbon, nitrogen and other direct riverine exports into the Clyde estuary. The horizontal flux models for these exports are included in Table 5 based on volumetric flow rate (Q) in $m^3\ s^{-1}$. The annual export, based on flow data for the survey period (1-Jan-20 to 31-Dec-21) is included in the final column of Table 5. This estimate only includes fluxes attributed to continuous point or diffuse sources. Sporadic pollution from winter road salting or periodic agricultural fertiliser application is estimated separately.

Storm events dominated riverine loading of DOC and nutrients from agricultural run-off and low water levels dominated inputs from point

Table 4
Categorisation of the dominant sources of GHG and nutrients between point and diffuse sources and their dependence on flow in upper and lower Clyde catchment.

		Upper catchment dominant source		Lower catchment dominant source	
		Point	Diffuse	Point	Diffuse
Flow	**Independent of flow**		Cl^-, Na^+ [4]	CH_4, TP, NH_4^+ (TDN, N_2O, CO_2)[1]	Cl^-, Na^+ [4] NO_3^-, N_2O, CO_2
	Influenced by flow	DIC, SO_4^{2-}, Ca^{2+}, Mg^{2+} [2]	CH_4, N_2O, CO_2 [3], DOC TP, TDN, NO_3^-, NH_4^+, K^+	DIC, SO_4^{2-}, Ca^{2+}, $Mg^{2,+}$ [2]	TDN, K^+, DOC

Notes.
[1] Point sources independent of flow are only evident in the lower (urban) catchment and all GHGs are influenced by this type of source. Values in brackets are significant sources not the dominant source.
[2] Point sources influenced by flow (DIC, SO_4^{2-}, Ca^{2+}, Mg^{2+}) are related to groundwater inputs. This type of source occurs in both the upper and lower catchment for this group of ions. Ions concentrations increase by an order of magnitude between the upper and lower catchment. This can be attributed (due to extensive further investigation by the authors) to mine water outflows from disused coal mines, which is a feature of the middle and lower Clyde catchment. Rainfall influences both the water residence time within the mine system and source flow rate influence the point source characteristics.
[3] Diffuse sources where the concentration increases with flow, such as for DOC are dominated by storm runoff events (Vaughan et al., 2017). GHGs in the upper catchments behave similarly to nutrient suggesting a similar source, however in the lower catchment point sources dominate GHG concentrations to the extent that for CH_4 diffuse generation is difficult to detect.
[4] Diffuse sources where the concentrations are independent of flow are exhibited by Cl^- and Na^+, throughout the catchment. Salt in river water is typically found to be damped by the catchment and independent from atmospheric inputs. (Neal and Kirchner, 2000). This type of analysis does not account for period inputs such as those caused by winter road salting.

sources, particularly those near to measurement locations. Variability in this relationship does arise due to hysteresis. For example DOC concentrations during storm events are related to the whether the DOC source is plentiful or exhaustible (Vaughan et al., 2017; Vaughan and Schroth, 2019 and Pohle et al., 2021). In this study continuous measurements were not available, resulting in the inability to quantify any hysteresis.

The annual loss of TDC from DIC, TOC, CO_2 and CH_4, to the estuary was estimated as 48.39 ± 3.6 Gg C yr^{-1}, with annual DIC export approximately double that of DOC and four times that of CO_2, with CH_4 accounting for 0.03%. The annual loss of total nitrogen, from TDN and N_2O, to the estuary was estimated as 4.03 ± 0.38 Gg N yr^{-1} of which N_2O represents 0.06%. The largest exports are for TDC, Cl^-, SO_4^{2-}, Ca^{2+}, all exceeding 40 Gg yr^{-1}, with Na^+ exceeding 36 Gg yr^{-1}, with road winter salting contributing an additional 10 Mg yr^{-1} of Cl^- and 5.6 Mg yr^{-1} of Na^+.

Despite the focus on measuring DOC in rivers, a recent UK modelling study demonstrated that DIC accounted for 80% of the TDC flux from the UK's 7 largest rivers (Jarvie et al., 2017) and a one-year study (2017) measured DIC as 78% of the TDC flux for the same rivers (Tye et al., 2022). Table 6 provides a ranked comparison of DIC and DOC export from various UK rivers, including the River Clyde from this study, based on river catchment area on a per annum basis, showing the dominance of DIC export over DOC in the UK.

4. Discussion

4.1. Urban nutrients and climate warming increase GHG emissions

Our study supports the growing global concern that GHG emissions from water bodies are increasing because of the interaction between nutrient levels and climate warming. More specifically our study points to the largest increase in riverine GHGs coming from urban nutrients and the riverine climate stressors of low summer water levels resulting in increased water residence times and reduced river oxygenation. Our source-to-sea methodology showed clearly that seasonal patterns of CH_4, CO_2 and N_2O changed between the semi-natural environment in the upper catchment and urban environment in the lower catchment. In the semi-natural upper catchment GHGs were higher in winter, while in the lower urban catchment, GHG were significantly higher in summer. The GHGs from the urban catchment were dominated by point source inputs and their impact increased during low river flow and high temperature conditions. In the agricultural middle catchment GHG concentrations increased slightly above those of the semi-natural upper catchment but did not exhibit a change in seasonal pattern. This seasonal change in GHG concentrations may be related to changes in microbial community composition and activities, which have been observed downstream of UWWTP (Y. Zhou et al., 2022; Beaulieu et al., 2010). The abundance of sediment microbial community have been found to be correlated with EC, organic matter, TP, DO and TN (Feng et al., 2022). This suggests microbial adaptation to changing conditions.

Riverine dissolved GHG, nutrient and chemical concentrations all increased from source-to-sea, in line with the increasing percentage of urban and agricultural land cover. The increase in GHG concentrations between the semi-natural and urban environment was on average three times higher for N_2O and CO_2, but twenty times higher for CH_4, suggesting the significant nature of CH_4 as an urban marker. While there were few significant correlations for any GHGs in the upper catchment, in the lower urban catchment strong correlations occurred between all GHGs and water physiochemical properties, suggesting that removal of contaminates from river systems, could lower GHG concentrations. Three main anthropogenic sources were identified that increased GHGs these included: (1) UWW outflows as a major point source of both CH_4 linked to TP and TDN, and N_2O linked to TDN; (2) MW outflows as a major point source of CH_4 and CO_2 emanating from groundwater interacting with disused coal mines and (3) agricultural activities as a major diffuse source of N_2O linked to TDN. Additionally, three major hydrological-environmental interactions were found that increased GHG concentrations in addition to those directly attributed to the nutrient increases. These included: (1) low oxygen conditions, (2) higher temperatures and (3) changes in river geometry linked to increased water residence times, and made it challenging to attribute causes absolutely.

4.2. High nutrient-residence time interactions promote GHG generation

Once the availability of TDN is accounted for (N_2O/TDN) neither T_w (in the range 0–22°C) or DO% (>90%) have significant effects on N_2O concentration. However where water residence time increases, T_W and DO% appear significant. In low flow situations, residence time is further increased, decreasing DO% and providing more time for temperatures to increase in summer. Both this increased residence time (Zarnetske et al., 2011) and low oxygen level (Frey et al., 2020; Rosamond et al., 2012) will act to increase N_2O, by promoting dentification and increasing the proportion of N_2O per unit TDN.

In the upper Clyde catchment CH_4 concentrations are low and highly variable, with higher CH_4 observed with elevated DOC occurring in high flow events, suggesting DOC availability may be limiting CH_4. However in the lower urban catchment CH_4 is strongly positively correlated to T_W, TP, TDN and DIC and negatively correlated with flow and DO%. This point source CH_4 generation is over 20 times higher than that derived

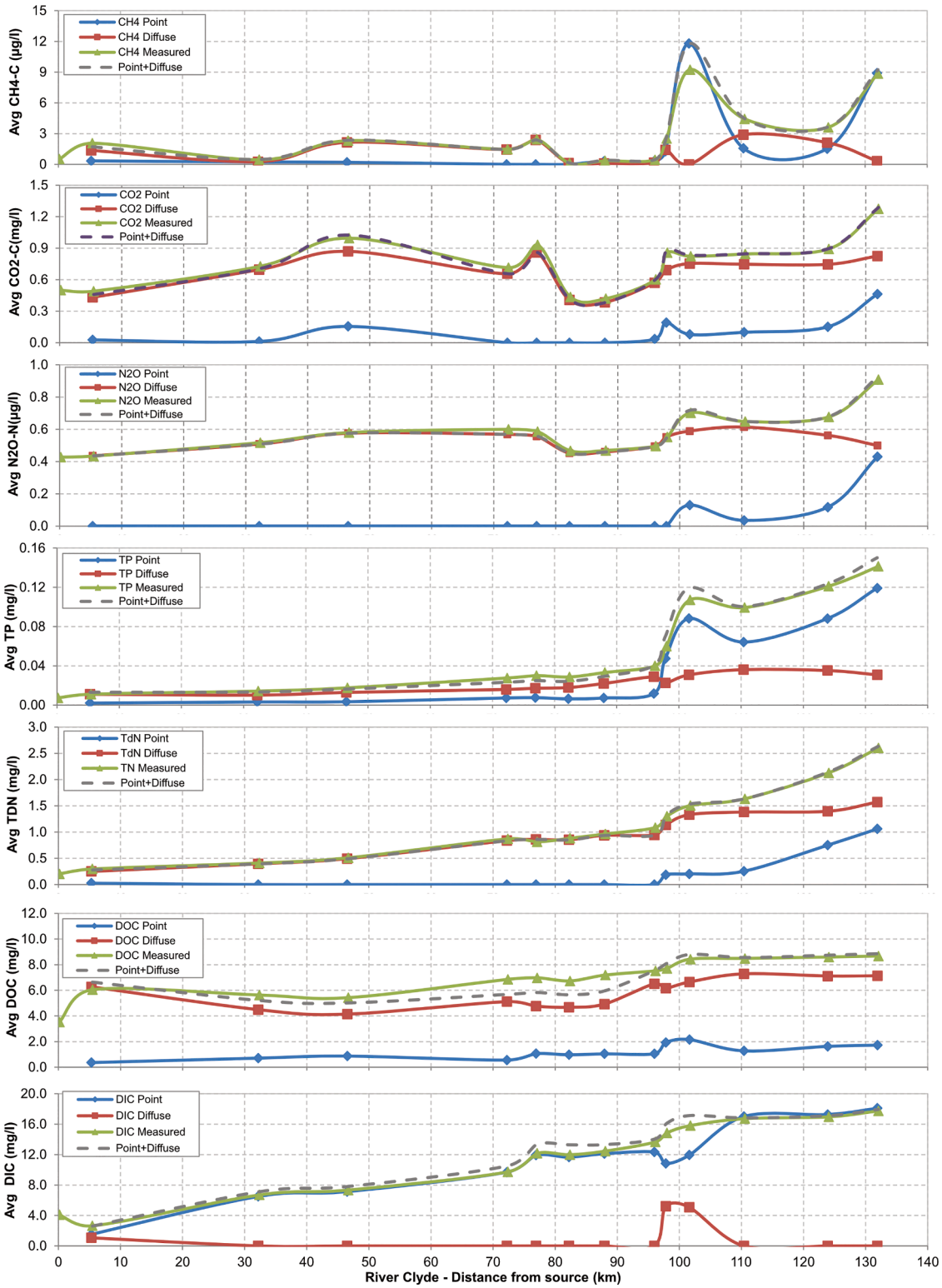

Fig. 8. Average concentrations from point source and diffuse sources on the River Clyde, The concentrations for measured data and determination of point and diffuse sources are shown for: CH_4, CO_2, N_2O, TP, TDN, DOC and DIC, against distance from source (C2 at 0 km to C26 at 134 km). For other ions supplementary data Figure A6. The measured concentrations are the average values measured across the 21 surveys for each location. The point and diffuse concentrations are the average values based on the 2 year of flow data for the time of the survey (1st January 2020 to 31st December 2021) applied at 15-minute intervals. Considerable input from point sources for both nutrients and GHG occurs after a distance of 95 km and is coincident with an increase in urban land cover and the three highly urban tributaries entering the River Clyde.

Table 5
Flux of CO_2, CH_4, N_2O, TP, TDN, DOC, DIC, Cl^-, NO_3^-, SO_4^{2-}, Na^+, NH_4^+, K^+,Ca^{2+}, Mg^{2+}into the Clyde Estuary.

Flux	Concentration equations (Q is in $m^3 s^{-1}$) $CT = A . Q^{(B-1)} + C . Q^{(D-1)}$	R^2	P-value	Annual export (tonnes)
F_{DOC} (mgl^{-1})	$= 36.0526 . Q^{-1} + 0.4979 . Q^{0.6940559}$	0.425	<0.005	13,534 ± 1510
F_{DIC} (mgl^{-1})	$= 60.70614. Q^{-0.36701}$	0.891	<0.001	27,629 ± 1448
F_{TDN} (mgl^{-1})	$= 22.1784 . Q^{-1} + 1.5727$	0.819	<0.001	4023 ± 377
F_{CO2_C} (mgl^{-1})	$= 9.66653 . Q^{-1} + 0.825557$	0.781	<0.001	7213 ± 654
F_{CH4_C} (μgl^{-1})	$= 184.1654 . Q^{-1} + 0.000000394 . Q^{2.93923}$	0.798	<0.001	14.4 ± 3.3
F_{N2O_N} (μgl^{-1})	$= 13.291247 . Q^{-1} + 0.07187. Q^{0.38284}$	0.753	<0.001	2.3 ± 0.14
F_{TP} (mgl^{-1})	$= 2.490657. Q^{-1} + 0.000132 . Q^{1.31679}$	0.964	<0.001	229 ± 36
F_{Cl^-}($\mu moll^{-1}$)	$= 8303.752 . Q^{-1} + 494.1491$	0.719[(1),(2)]	<0.001	48,273 ± 5186
$F_{NO_3^-}$($\mu moll^{-1}$)	$= 1533.528 . Q^{-1} + 74.2137$	0.773	<0.001	13,978 ± 1543
$F_{SO_4^{2-}}$($\mu moll^{-1}$)	$= 1140.427 . Q^{-0.430324}$	0.744	<0.001	40,968 ± 3778
F_{NA^+}($\mu moll^{-1}$)	$= 10,460.07 . Q^{-1} + 524.7421$	0.837[(1),(2)]	<0.001	36,001 ± 5734
$F_{NH_4^+}$($\mu moll^{-1}$)	$= 139.6026 . Q^{-1} + 11.07243$	0.342	<0.001	498 ± 62
F_{K^+}($\mu moll^{-1}$)	$= 863.9982 . Q^{-1} + 55.69099 . Q^{1.00091}$	0.927[(2)]	<0.001	5805 ± 474
$F_{Ca^{2+}}$($\mu moll^{-1}$)	$= 1986.658 . Q^{-0.31986}$	0.841	<0.001	42,040 ± 3376
$F_{Mg^{2+}}$($\mu moll^{-1}$)	$= 1349.282 . Q^{-0.421596}$	0.873[(2)]	<0.001	12,598 ± 1412

Notes:
(1) $CT = CP + CD$, where $CP = A.Q^{(B-1)}$ and $CD = C.Q^{(D-1)}$ (C = concentration, *T* = Total, *P* = Point, *D* = Diffuse).
(2) Two values removed for January 21 and February 21 and assumed due to winter salting, as salt evident on the roads
(3) One value removed for August 2021 due to tidal ingress at Glasgow green, this most influenced K^+ $Mg^{2+}$$Na^+$and Cl^-concentrations.

from diffuse sources. Generation of CH_4 in the lower urban catchment may be linked to eutrophication (nutrient enrichment). Our $SUVA_{254}$ values show a shift in riverine OC sources toward a more microbial and algal origin, as has been found as human disturbance increases (Lambert et al., 2017). High CH_4 in many shallow lakes is produced by eutrophication, mostly driven by TP and TDN enrichment and sediment microbiome (Davidson et al., 2018; Aben et al., 2017; Nijman et al., 2022). This mechanism is less likely in river ecosystem due to continual flushing, but during low water levels, increased residence times in combination with the high nutrient concentrations from UWW appear responsible for eutrophication and significant CH_4 generation. This may be enabled by electron donor availability in the receiving waters. This effect was most exacerbated when water residence times were further increased by the flow restriction at the tidal weir.

4.3. Main uncertainty in the causes of GHG variation

Greenhouse gas concentrations were inversely correlated with river oxygenation. This correlation was influenced by several mechanisms, where the dominance changed with position in the catchment. High turbulence caused oxygenation of the water and outgassing of the supersaturated GHGs. Respiration, photosynthesis and decomposition can create inverse relationships between oxygen and CO_2 dependant on their balance in the water column (Aho et al., 2021). Low oxygen conditions can result in anaerobic condition, promoting both methanogenesis and denitrification, which increase CH_4 and N_2O production respectively, from the available resources. While turbulence outgasses GHGs to

Table 6
Comparison of DIC and DOC export from UK Rivers as a function of catchment area.

River	Catchment Size (km^{-2})	DIC export Mg km^{-2} yr^{-1}	DOC export $Mgkm^{-2}yr^{-1}$	Ratio DIC/DOC	
Halladale	193	1.0	13.06	0.1	(García-Martín et al., 2021), (Tye et al., 2022)
Conwy	340	3.9	12.15	0.3	(García-Martín et al., 2021), (Tye et al., 2022)
Forth	1025	9.4	11.41	0.8	(García-Martín et al., 2021), (Tye et al., 2022)
Tay	5042	5.4	4.91	1.1	(García-Martín et al., 2021), (Tye et al., 2022)
Tamar	956	9.0	7.64	1.2	(García-Martín et al., 2021), (Tye et al., 2022)
Tay	4587	6.8	5	1.4	(Jarvie et al., 2017)
Tyne	2262	9.25	4.93	1.9	(García-Martín et al., 2021), (Tye et al., 2022)
Dart	257	8.9	5.18	1.7	(García-Martín et al., 2021), (Tye et al., 2022)
Kelvin	331	9.25	4.93	1.9	(Gu et al., 2021)
River Clyde	2003	13.78	6.74	2.0	This Study
Clyde	2003	13.5	6.04	2.2	(García-Martín et al., 2021), (Tye et al., 2022)
Clwyd	431	12.7	5.17	2.5	(García-Martín et al., 2021), (Tye et al., 2022)
Tweed	4390	8.3	2.9	2.9	(Jarvie et al., 2017)
Yorkshire Ouse	3315	16.2	4.3	3.8	(Jarvie et al., 2017)
Severn	9895	14	3.3	4.2	(Jarvie et al., 2017)
Trent	8231	17.7	2.4	7.4	(Jarvie et al., 2017)
Humber-Trent	8209	14.6	1.77	8.2	(García-Martín et al., 2021), (Tye et al., 2022)
Ely Ouse	3430	10.6	1.2	8.8	(Jarvie et al., 2017)
Thames	9948	13.4	1.4	9.6	(Jarvie et al., 2017)
Thames	9948	9.3	0.57	16.3	(García-Martín et al., 2021), (Tye et al., 2022)
Avon	1712	18.5	0.86	21.5	(García-Martín et al., 2021), (Tye et al., 2022)
Test	1035	19.3	0.51	37.8	(García-Martín et al., 2021), (

(*continued on next page*)

Table 6 (*continued*)

River	Catchment Size (km^{-2})	DIC export Mg km^{-2} yr^{-1}	DOC export $Mgkm^{-2}yr^{-1}$	Ratio DIC/ DOC	
					Tye et al., 2022)
Average export		11.1	4.9	2.4	
Catchment weighted Average export		12.32	2.98	4.1	

Note
[1]Load of dissolved inorganic carbon (DIC) and dissolved organic carbon (DOC) for the significant British rivers as function of catchment area as a comparator for the river Clyde.
[2]DOC exports are from (García-Martín et al., 2021) and DIC exports estimated from (Tye et al., 2022), but data in these papers was gathered as part of the same study.

atmosphere it also produces conditions less likely to promote CH_4 and N_2O production making it difficult to fully distinguish the mechanisms. The lower urban river has the highest correlations, with GHGs increasing exponentially with reducing oxygen levels. The oxygen concentration primarily influences CH_4, while CO_2 and N_2O are influenced by the DO% (CH_4 $R^2 = 0.45$, CO_2 $R^2 = 0.74$, N_2O $R^2 = 0.24$ (P-value > 0.001)), suggesting CH_4 generation is less influenced by temperature.

Summer seasonal changes impact both temperature and rainfall, which together impact GHG concentrations. Lower rainfall reduces river flow and diffuse nutrients inputs and increases the impact of point source inputs. Higher temperatures reduce the available oxygen, due to reduced solubility and can increase microbial activity. As flow and temperature are often highly correlated this can make distinguishing these mechanisms difficult. Many researchers suggest temperature is a major effect (Wang et al., 2021; Herrero Ortega et al., 2019 and Rosentreter et al., 2021). However, this study found that the size of the impact of flow and temperature on GHG concentrations is dependant on the location in the catchment and specifically the balance between diffuse and point source inputs. The upper catchment is dominated by diffuse inputs, which increase in higher flow and correspond to an increase in GHG concentrations. The lower urban catchments is dominated by point source inputs and corresponds to an increase in GHG concentrations with low flow. Flow and hence nutrient concentrations being more significant than direct impact of temperature in accounting for GHG variability. After flow, TP is the major influence on CH_4 and TDN on N_2O. The use of the load appointment model to distinguish between points and diffuse sources of GHGs and nutrients suggests that nutrients, however they are delivered, are dominating GHG production. Fully distinguishing between temperature and flow impacts would require longer data set with more instances of high flow during the summer.

Changes in river geometry that reduce river velocity and increase water residence times also cause deposition of sediments and nutrients and reduce oxygen saturation. River sections with increased residence time exhibited higher GHG concentrations, with the largest increases occurring in low flow conditions. However, proportioning the cause of this increase between; increased residence time, reduced outgassing due to lower turbulence, lower oxygen conditions, or deposition of sediments and nutrients as a source of GHG production is challenging. These higher residence time river sections act as point source locations for GHG generation compared to the surrounding river with CH_4 concentrations showing the most significant increase suggesting the creation of anaerobic sediments may be the most significant impact.

Our results show an increase in GHGs, particularly CH_4, in the receiving river after UWWTPs, with the riverine CH_4 concentrations dominated by point source characteristics, pointing to the UWWTP inflows as causal. UWWTP generate CH_4, in locations such as sewer pipes and primary sedimentation, although CH_4 was not noted as discharged in effluent water (Masuda et al., 2018). We made measurements of GHG concentrations in some UWWTPs outflows, which were low in dissolved GHG including CH_4, and this suggested that CH_4 was generated within the receiving river due to changes in the river physicochemical properties, including nutrient availability, rather than transferred from the UWWTP. However, we made insufficient measurements in UWWTP outflows, due to their inaccessibility, to confirm this absolutely. Unexplained CH_4 concentrations in the stream sections after UWW treatments works in southwest Germany were attributed to in-water generation due to additional organic carbon load in the effluent water (Alshboul et al., 2016). After hydrology was accounted for TP, also dominated by point source characteristics, had the highest correlation with unexplained CH_4 concentrations (TP $R^2 = 0.59$ at C26), although this correlation changed with proximity to UWWTP. Other authors indicated correlations between TP and CH_4 concentrations, in urban settings usually by impacting microbial activity (Zhang et al., 2021; Martinez-Cruz et al., 2017; Hao et al., 2021).

4.4. Carbon dioxide concentration variability reduced by carbonate buffering

Concentrations of CO_2 were less variable than those of N_2O and CH_4, mostly driven by diffuse sources, with point source inflows associated with tributaries receiving MW, causing short-term CO_2 increases. In-stream mineralization of DOC, the most likely generation mechanism for the consistent super-saturation of CO_2, would require a constant input of carbon to sustain CO_2 supersaturation levels (Winterdahl et al., 2016). DOC concentrations varied little through the catchment emanating from diffuse input, while DIC increased from source-to-sea, dominated by MW inflows. These MW inflows added significant amounts of DIC from the dissolution of limestone, producing high alkalinity, and many dissolved contaminates. The MW inflows are supersaturated with CO_2, which outgases very rapidly in treatment cascades or headwater streams. This rapid outgassing was observed to shift the pH upwards creating a new carbonate equilibrium. This changing equilibration would convert some of the remaining CO_2 to bicarbonate rather than emitting it to the atmosphere, thus reducing the gradient of CO_2 across the air-water interface (Stets et al., 2017). Aquatic primary productivity produces oxygen and consumes CO_2. However, primary productivity can be maintained with diminished CO_2, in high alkalinity waters by converting bicarbonate to CO_2 to support productivity (Aho et al., 2021). Conversely mineralisation of DOC to CO_2 would change the carbonate balance increasing bicarbonate concentrations. It is likely that this significant carbonate buffering available in the Clyde is responsible for the low variability in CO_2 concentrations and the reason why nutrients rather than carbon availability appear to influence CO_2 concentrations.

4.5. Acid mine inflows are a major source of GHG

In the middle and lower catchment tributaries, high concentrations of both CO_2 and CH_4 occurred linked to outflows from disused coal mine adits. Where carbonate rock is present, and much coal bearing strata in the UK is associated with Carboniferous limestone (British Geological Survey, 2022), the sulphuric acid generated in the mine dissolves the calcium carbonate to produce CO_2 (Hedin and Hedin, 2016; Vesper et al., 2016; Jarvis, 2006). Details of CH_4 released in MW have not, to our knowledge, been published. Most GHGs from MW had out-gassed before reaching the River Clyde. However high CO_2 and CH_4 concentrations in T10 were traced back to several MW inflows. These MW inflows had high concentrations of DIC, SO_4^{2-}, Ca^{2+}, Mg^{2+} and K^{+}, which together acted as a marker for legacy coal mining. Many other MW sources were traced in the catchment with this marker, although not included within this publication. Despite the focus on measuring DOC in rivers, our data suggest that for the River Clyde carbon loss is dominated

by DIC, with the annual DIC export approximately double that for DOC. Comparison with other riverine studies demonstrated that DIC is the major component of the dissolved carbon in UK Rivers, with DIC accounting for 70 to 80% of carbon loss (Table 6). Our results suggest that the anthropogenic impacts of disused coal mines are accelerating carbon loss.

4.6. Legacy industry is still detectable in our rivers

Other increases in ion concentrations and pH were identified in the three most urban tributaries (T19, T22 and T23). Urban tributaries T19 and T22, had the highest concentrations of DIC, SO_4^{2-}, Ca^{2+}, Mg^{2+} and K^+, attributed to inflows of MW from legacy coal mining. Both tributaries had legacy iron or steel making near to the rivers and may have iron slag buried within the catchment (Historic Environment Scotland, 2022). Steel slag is known to increase pH, alkalinity, and Ca^{2+} concentration (Riley and Mayes, 2015). The urban tributary T23, had the highest concentrations of Na^+ and SO_4^{2-} probably associated with leachate from legacy paper production (Skinner, 1939). T22 also experienced the highest Na^+ and Cl^- ion concentrations in the winter likely from winter road salting, as this tributary has the biggest road network, including a motorway. Data suggests that road drainage is entering the river directly adding an estimated 15 Mg yr^{-1} of NaCl.

5. Conclusions

5.1. Benefits of a source-to-sea approach in interpreting riverine GHGs

We have used the Clyde catchment, with its transitioning land cover from semi-natural through agricultural and legacy industrial to highly urban as a source-to-sea study to support identification of GHG sources. This source-to-sea investigative approach was found effective in tracing how changes in the nature and size of the riverine environment impacted GHG concentrations, particularly as GHGs were not conserved but outgased in turbulent riverine sections. This variable outgassing makes correlations on a catchment scale misleading and is probably one reason for the high variability in GHG-to-nutrient relationships reported in the literature. A key aspect of GHG source identification included the use of load appointment modelling to distinguish point and diffuse sources by their degree of dependence on flow. This was effective in confirming diffuse GHG sources from agriculture and point GHG sources from UWW and MW. This load appointment modelling approach enabled two main seasonal impacts, high temperature and low water levels, to be distinguished. Analysis suggested that the impact of low water levels dominated over temperature change and failure to account for changing water levels, with their implications for oxygen and residence times, may account for some of the variability in the impact of temperature on GHG generation reported in the literature.

Measurement of a high number of water physiochemical properties allowed source fingerprinting of different inflows, which enabled detection even when the inflows were not physically identified, supporting identification of contamination from legacy industry. Results suggested that outflows from UWW treatment plants caused generation of GHG within the riverine water column. Changes in the seasonal pattern of GHG generation associated with urban wastewater inflows could be due to changes in microbial community structure, eutrophication at low water levels and supported by the availability of electron donors and acceptors in receiving waters. This was not confirmed as part of this study, and it is suggested that future surveys should be designed to quantify in-water generation resulting from mixing of UWW and riverine water.

The most important anthropogenic GHG from inland waters is CH_4 (Rosentreter et al., 2021), but CH_4 outgases the most rapidly, due to its high concentration to solubility ratio, as such catchment scale analysis can be misleading. Improved methods to detect and quantify CH_4 concentrations are required. A drone-mounted CH_4 sensor might be effective in identifying point sources while continuous in-situ CH_4 measurements would better define source-flow relationships, although sensor reliability and sensitivity needs improvement. Where the source of nutrient pollution is unclear, human tracers such as caffeine could be applied to support understanding of contributions to nutrient pollution (Mizukawa et al., 2019, and Chen et al., 2002).

5.2. Implications and ideas for policy makers

To effectively reduce anthropogenic GHGs from the riverine environment it is important to understand their sources. For the River Clyde, UWW outflows were a major point source of both anthropogenic CH_4 and N_2O, MW outflows a major point source of anthropogenic CH_4 and CO_2 and agricultural activities (including field and farmyard run-off and poorly maintained septic tanks (septic tank are not effective in removing nitrogen and phosphorous (O'Keeffe et al., 2015)) were a source of anthropogenic N_2O. All sources of GHGs were associated with high concentrations of nutrients. Hence reducing nutrient loading, industrial and legacy contamination and agricultural run-off would ultimately act to reduce GHGs within riverine environments. Pollution point sources are easier to tackle as the location of the inflows are known.

While many UWWTP in the Clyde have phosphorous removal, our measurements suggest that levels of effectiveness vary between plants, suggesting improvement is possible. Additionally none of the UWWTP in this area have nitrogen removal (European Commission (Directorate General Environment), 2016). Riverine environments with low oxygenation, increased river residence times and high levels of nitrogen, should be prioritised for nitrogen removal from UWWTP to have the largest impact on N_2O reduction. Urban influences may have stimulated adaptation in microbial communities, further increasing GHG production, and further studies of microbial activity may support GHG reduction. Nitrogen capture at UWWTP could ultimately act as an important source of fertiliser, avoiding outflows to the environment (van der Hoek et al., 2018). Mine water is more difficult to tackle in terms of GHG generation as GHGs are generated below ground with the generation mechanism poorly understood.

While agricultural pollution was primarily from diffuse sources additional measurements showed a significant proportion entered the Clyde via the numerous field drainage ditches and small streams, which could be treated as point sources. Approaches to reduce run-off may include: (1) use freshwater wetlands for nitrogen and phosphorus removal (Land et al., 2016) and wetlands have been shown as effective for diffuse run-off (Ockenden et al., 2012); (2) use of biochar filtration, an effective technology for both cleaning of wastewater and run-off water. Its capabilities include removal of pesticides, organic chemicals and nutrients. However, a practical approach for application to small streams is needed. After use the biochar could be redeployed onto farmland supporting carbon sequestration and a circular economy, recycling nutrients and further preventing run-off (Catizzone et al., 2021; Phillips et al., 2022; Kamali et al., 2021); (3) Riparian buffer zones are recommended between crops and rivers. In Scotland, General Binding Rule 20 requires a buffer strip at least 2 m wide to be left between surface waters and wetlands and cultivated land (SEPA, 2009). This rule was not set with the objective of reducing nutrient leeching. Further research demonstrates that woody vegetation is more effective than shrubs or grass at preventing nutrient leaching to rivers, with a 60 m buffer strip effectively removing all nutrients (Aguiar et al., 2015). While this would take considerable agricultural land, approximately 70% of nutrients are removed by a 12 m strip, which would also stabilise river banks, reduce erosion and sediment loss, increase biodiversity and provide shade making the riverine system more robust to climate change (Cole et al., 2020).

Declaration of Competing Interest

The authors declare that they have no known competing financial

interests or personal relationships that could have appeared to influence the work reported in this paper.

Data availability

The data used for this manuscript has been published by the Environmental Information Data Centre at https://eidc.ac.uk/ (Brown et al., 2023).

Acknowledgements

This work was financially supported by a Natural Environment Research Council (NERC) studentship through the IAPETUS 2 Doctoral Training Partnership, Grant No. NE/S007431/1.

The authors would like to thank the three anonymous reviewers who helped improve the quality of the manuscript.

Supplementary materials

Supplementary material associated with this article can be found, in the online version, at doi:10.1016/j.watres.2023.119969.

References

Aben, R.C.H., Barros, N., Van Donk, E., Frenken, T., Hilt, S., Kazanjian, G., Lamers, L.P. M., Peeters, E.T.H.M., Roelofs, J.G.M., De Senerpont Domis, L.N., Stephan, S., Velthuis, M., Van De Waal, D.B., Wik, M., Thornton, B.F., Wilkinson, J., Delsontro, T., Kosten, S., 2017. Cross continental increase in methane ebullition under climate change. Nat. Commun. 8 (1), 1–8. https://doi.org/10.1038/s41467-017-01535-y.

Abril, G., Borges, A.V., 2019. Ideas and perspectives: carbon leaks from flooded land: do we need to replumb the inland water active pipe? Biogeosciences 16 (3), 769–784. https://doi.org/10.5194/bg-16-769-2019.

Aguiar, T.R., Asera, K., Parron, L.M., Brito, A.G., Ferreira, M.T., 2015. Nutrient removal effectiveness by riparian buffer zones in rural temperate watersheds : the impact of no-till crops practices. Agric. Water Manag. 149, 74–80. https://doi.org/10.1016/j.agwat.2014.10.031.

Aho, K.S., Hosen, J.D., Logozzo, L.A., McGillis, W.R., Raymond, P.A., 2021. Highest rates of gross primary productivity maintained despite CO2 depletion in a temperate river network. Limnol. Oceanogr. Lett. 6 (4), 200–206. https://doi.org/10.1002/lol2.10195.

Alshboul, Z., Encinas-Fernández, J., Hofmann, H., Lorke, A., 2016. Export of dissolved methane and carbon dioxide with effluents from municipal wastewater treatment plants. Environ. Sci. Technol. 50 (11), 5555–5563. https://doi.org/10.1021/acs.est.5b04923.

Beaulieu, J.J., Shuster, W.D., Rebholz, J.A., 2010. Nitrous oxide emissions from a large, impounded river: the Ohio river. Environ. Sci. Technol. 44 (19), 7527–7533. https://doi.org/10.1021/es1016735.

Beaulieu, J.J., Tank, J.L., Hamilton, S.K., Wollheim, W.M., Hall, R.O., Mulholland, P.J., Peterson, B.J., Ashkenas, L.R., Cooper, L.W., Dahm, C.N., Dodds, W.K., Grimm, N.B., Johnson, S.L., McDowell, W.H., Poole, G.C., Maurice Valett, H., Arango, C.P., Bernot, M.J., Burgin, A.J., Crenshaw, C.L., Helton, A.M., Johnson, L.T., O'Brien, J. M., Potter, J.D., Sheibley, R.W., Sobota, D.J., Thomas, S.M., 2011. Nitrous oxide emission from denitrification in stream and river networks. Proc. Natl. Acad. Sci. U. S. A. 108 (1), 214–219. https://doi.org/10.1073/pnas.1011464108.

Borges, A.V., Darchambeau, F., Lambert, T., Bouillon, S., Morana, C., Brouyère, S., Hakoun, V., Jurado, A., Tseng, H.C., Descy, J.P., Roland, F.A.E., 2018. Effects of agricultural land use on fluvial carbon dioxide, methane and nitrous oxide concentrations in a large European river, the Meuse (Belgium). Sci. Total Environ. 610–611, 342–355. https://doi.org/10.1016/j.scitotenv.2017.08.047.

Bosse, U., Frenzel, P., Conrad, R., 1993. Inhibition of methane oxidation by ammonium in the surface layer of a littoral sediment. FEMS Microbiol. Ecol. 13 (2), 123–134. https://doi.org/10.1016/0168-6496(93)90030-B.

Bowes, M.J., Smith, J.T., Jarvie, H.P., Neal, C., 2008. Modelling of phosphorus inputs to rivers from diffuse and point sources. Sci. Total Environ. 395 (2–3), 125–138. https://doi.org/10.1016/j.scitotenv.2008.01.054.

British Geological Survey: BGS geology viewer, 2022.

Broder, T., Blodau, C., Biester, H., Knorr, K.H., 2012. Peat decomposition records in three pristine ombrotrophic bogs in southern Patagonia. Biogeosciences 9 (4), 1479–1491. https://doi.org/10.5194/bg-9-1479-2012.

Brown, A., Van Dijk, N., Pickard, A.E., 2023. Greenhouse gas and water chemistry measurements for the Clyde river, tributaries and estuary, 2021-2022. Environ. Inf. Data Cent. https://doi.org/10.5285/c3527258-c9ab-40d9-af0c-ddedabbd67a1.

Catizzone, E., Sposato, C., Romanelli, A., Barisano, D., Cornacchia, G., Marsico, L., Cozza, D., Migliori, M., 2021. Purification of wastewater from biomass-derived syngas scrubber using biochar and activated carbons. Int. J. Environ. Res. Public Health.

Chen, Z., Pavelic, P., Dillon, P., Naidu, R., 2002. Determination of caffeine as a tracer of sewage effluent in natural waters by on-line solid-phase extraction and liquid chromatography with diode-array detection. Water Res 36, 4830–4838.

Ciais, P., Sabine, C., Bala, G., Bopp, L., Brovkin, V., Canadell, J., Chhabra, A., DeFries, R., Galloway, J., Heimann, M., Jones, C., Quéré, C.Le, Myneni, R.B., Piao, S., Thornton, P., 2013. Carbon and other biogeochemical cycles. In: climate change 2013. In: Stocker, T.F., Qin, D., Plattner, G.-K., Tignor, M., Allen, S.K., Boschung, J., Nauels, A., Xia, Y. (Eds.), The Physical Science Basis. Contribution of Working Group I to the Fifth Assessment Report of the Intergovernmental Panel on Climate Change, edited by V. B. and P. M. M. Cambridge University Press, Cambridge, United KingdomNew York, NY, USA.

Clyde River Foundation: The Clyde catchment, [online] Available from: https://www.clyderiverfoundation.org/clyde-catchment/, 2020.

Cole, L.J., Stockan, J., Helliwell, R., 2020. Agriculture, Ecosystems and Environment Managing riparian buffer strips to optimise ecosystem services : a review. Agric. Ecosyst. Environ. 296 (April), 106891 https://doi.org/10.1016/j.agee.2020.106891.

Cotovicz, L.C., Ribeiro, R.P., Régis, C.R., Bernardes, M., Sobrinho, R., Vidal, L.O., Tremmel, D., Knoppers, B.A., Abril, G., 2021. Greenhouse gas emissions (CO2 and CH4) and inorganic carbon behavior in an urban highly polluted tropical coastal lagoon (SE, Brazil). Environ. Sci. Pollut. Res. 28 (28), 38173–38192. https://doi.org/10.1007/s11356-021-13362-2.

Davidson, T.A., Audet, J., Jeppesen, E., Landkildehus, F., Lauridsen, T.L., Søndergaard, M., Syväranta, J., 2018. Synergy between nutrients and warming enhances methane ebullition from experimental lakes. Nat. Clim. Chang. 8 (2), 156–160. https://doi.org/10.1038/s41558-017-0063-z.

Dunfield, P., Knowles, R., 1995. Kinetics of inhibition of methane oxidation by nitrate, nitrite, and ammonium in a humisol. Appl. Environ. Microbiol. 61 (8), 3129–3135. https://doi.org/10.1128/aem.61.8.3129-3135.1995.

European Commission (Directorate General Environment): European commission urban waste water website: United Kingdom, [online] Available from: https://uwwtd.eu/United-Kingdom/(Accessed 23 December 2020), 2016.

Feng, W., Gao, J., Wei, Y., Liu, D., Yang, F., Zhang, Q., Bai, Y., 2022. Pattern changes of microbial communities in urban river affected by anthropogenic activities and their environmental driving mechanisms. Environ. Sci. Eur. 34 (1), 1–13. https://doi.org/10.1186/s12302-022-00669-1.

Frey, C., Bange, H.W., Achterberg, E.P., Jayakumar, A., Löscher, C.R., Arévalo-martínez, D.L., León-palmero, E., Sun, M., Sun, X., Xie, R.C., 2020. Regulation of nitrous oxide production in low-oxygen waters off the coast of Peru. Biogeosciences 17, 2263–2287.

Furukawa, Y., Inubushi, K., Furukawa, Y., 2004. Effect of application of iron materials on methane and nitrous oxide emissions from two types of paddy soils. Soil Sci. Plant Nutr. 50 (6), 917–924. https://doi.org/10.1080/00380768.2004.10408554.

García-Martín, E.E., Sanders, R., Evans, C.D., Kitidis, V., Lapworth, D.J., Rees, A.P., Spears, B.M., Tye, A., Williamson, J.L., Balfour, C., Best, M., Bowes, M., Breimann, S., Brown, I.J., Burden, A., Callaghan, N., Felgate, tacey L., Fishwick, J., Fraser, M., Gibb, S.W., Gilbert, P.J., Godsell, N., Gomez-Castillo, A.P., Hargreaves, G., Jones, O., Kennedy, P., Lichtschlag, A., Martin, A., May, R., Mawji, E., Mounteney, I., Nightingale, hilip D., Olszewska, J.P., Painter, S.C., Pearce, C.R., Pereira, M.G., Peel, K., Pickard, A., Stephens, J.A., Stinchcombe, M., Williams, P., Woodward, M.S., Yarrow, D., Mayor, D.J., 2021. Contrasting estuarine processing of dissolved organic matter derived from natural and human-impacted landscapes. Glob. Biogeochem. Cycles (2393175).

Garnier, J., Billen, G., Vilain, G., Martinez, A., Silvestre, M., Mounier, E., Toche, F., 2009. Nitrous oxide (N2O) in the Seine river and basin: observations and budgets. Agric. Ecosyst. Environ. 133 (3–4), 223–233. https://doi.org/10.1016/j.agee.2009.04.024.

Gómez-Gener, L., von Schiller, D., Marcé, R., Arroita, M., Casas-Ruiz, J.P., Staehr, P.A., Acuña, V., Sabater, S., Obrador, B., 2016. Low contribution of internal metabolism to carbon dioxide emissions along lotic and lentic environments of a Mediterranean fluvial network. J. Geophys. Res. Biogeosciences 121 (12), 3030–3044. https://doi.org/10.1002/2016JG003549.

Gu, C., Waldron, S., Bass, A.M., 2021. Carbon dioxide, methane, and dissolved carbon dynamics in an urbanized river system. Hydrol. Process. 35 (9), 1–17. https://doi.org/10.1002/hyp.14360.

Skinner, H.J., 1939. Waste problems in the pulp and paper industry. Ind. Eng. Chem. 31 (11), 1331–1335 [online] Available from: https://pubs.acs.org/doi/pdf/10.1021/ie50359a006#.

Hamilton, S.: Prediction of dissolved gas concentrations in water at atmospheric equilibrium, 3–6 [online] Available from: https://lter.kbs.msu.edu/docs/linx/linx2/linx2_dissolved_gas_headspace_equilibration_calcs.pdf, 2006.

Hao, X., Ruihong, Y., Zhuangzhuang, Z., Zhen, Q., Xixi, L., Tingxi, L., Ruizhong, G., 2021. Greenhouse gas emissions from the water–air interface of a grassland river: a case study of the Xilin River. Sci. Rep. 11 (1), 1–14. https://doi.org/10.1038/s41598-021-81658-x.

Hedin, R.S., Hedin, B.C., 2016. The complicated role of CO2 in mine water treatment. In: Proc. IMWA 2016, Freiberg/Germany, 3(TU), pp. 844–849.

Herlihy, A.T., Stoddard, J.L., Johnson, C.B., 1998. The relationship between stream chemistry and watershed land cover data in the mid-atlantic region. U.S., Water. Air. Soil Pollut. 105 (1–2), 377–386. https://doi.org/10.1023/A:1005028803682.

Herrero Ortega, S., Romero González-Quijano, C., Casper, P., Singer, G.A., Gessner, M.O., 2019. Methane emissions from contrasting urban freshwaters: rates, drivers, and a whole-city footprint. Glob. Chang. Biol. 25 (12), 4234–4243. https://doi.org/10.1111/gcb.14799.

Historic Environment Scotland: Canmore - clyde iron works, Canmore [online] Available from: https://canmore.org.uk/site/162565/glasgow-clyde-iron-works, 2022.

van der Hoek, J.P., Duijff, R., Reinstra, O., 2018. Nitrogen recovery from wastewater: possibilities, competition with other resources, and adaptation pathways. Sustain 10 (12). https://doi.org/10.3390/su10124605.

Hotchkiss, E.R., Hall, R.O., Sponseller, R.A., Butman, D., Klaminder, J., Laudon, H., Rosvall, M., Karlsson, J., 2015. Sources of and processes controlling CO2emissions change with the size of streams and rivers. Nat. Geosci. 8 (9), 696–699. https://doi.org/10.1038/ngeo2507.

Jarvie, H.P., King, S.M., Neal, C., 2017. Inorganic carbon dominates total dissolved carbon concentrations and fluxes in British rivers: application of the THINCARB model – Thermodynamic modelling of inorganic carbon in freshwaters. Sci. Total Environ. 575 (October), 496–512. https://doi.org/10.1016/j.scitotenv.2016.08.201.

Jarvis, A.P., 2006. The role of dissolved carbon dioxide in governing deep coal mine water quality and determining treatment process selection. In: 7th Int. Conf. Acid Rock Drain. 2006, ICARD - Also Serves as 23rd Annu. Meet. Am. Soc. Min. Reclam, 1, pp. 833–843. https://doi.org/10.21000/jasmr06020833.

Kamali, M., Appels, L., Kwon, E.E., Aminabhavi, T.M., Dewil, R., 2021. Biochar in water and wastewater treatment - a sustainability assessment. Chem. Eng. J. 420 (P1), 129946 https://doi.org/10.1016/j.cej.2021.129946.

Koschorreck, M., Prairie, Y.T., Kim, J., Marcé, R., 2021. Technical note: cO2is not like CH4- Limits of and corrections to the headspace method to analyse pCO2in fresh water. Biogeosciences 18 (5), 1619–1627. https://doi.org/10.5194/bg-18-1619-2021.

Lambert, T., Bouillon, S., Darchambeau, F., Morana, C., Roland, F.A.E., Descy, J.P., Borges, A.V., 2017. Effects of human land use on the terrestrial and aquatic sources of fluvial organic matter in a temperate river basin (The Meuse River, Belgium). Biogeochemistry 136 (2), 191–211. https://doi.org/10.1007/s10533-017-0387-9.

Land, M., Granéli, W., Grimvall, A., Hoffmann, C.C., Mitsch, W.J., Tonderski, K.S., Verhoeven, J.T.A., 2016. How effective are created or restored freshwater wetlands for nitrogen and phosphorus removal? A systematic review. Environ. Evid. 5 (1), 1–26. https://doi.org/10.1186/s13750-016-0060-0.

Liu, S., Raymond, P.A., 2018. Hydrologic controls on pCO2 and CO2 efflux in US streams and rivers. Limnol. Oceanogr. Lett. 3 (6), 428–435. https://doi.org/10.1002/lol2.10095.

Long, H., Vihermaa, L., Waldron, S., Hoey, T., Quemin, S., Newton, J., 2015. Hydraulics are a first-order control on CO2 efflux from fluvial systems. Geophys. Res. Biogeosciences 1912–1922. https://doi.org/10.1002/2015JG002955. Received.

Maavara, T., Lauerwald, R., Laruelle, G.G., Bouskill, N.J., Cappellen, P.Van, Regnier, P., 2019. Nitrous oxide emissions from inland waters : are IPCC estimates too high ? Glob. Chang. Biol. (July 2018) https://doi.org/10.1111/gcb.14504.

Martinez-Cruz, K., Gonzalez-Valencia, R., Sepulveda-Jauregui, A., Plascencia-Hernandez, F., Belmonte-Izquierdo, Y., Thalasso, F., 2017. Methane emission from aquatic ecosystems of Mexico City. Aquat. Sci. 79 (1), 159–169. https://doi.org/10.1007/s00027-016-0487-y.

Marx, A., Dusek, J., Jankovec, J., Sanda, M., Vogel, T., van Geldern, R., Hartmann, J., Barth, J.A.C., 2017. A review of CO2 and associated carbon dynamics in headwater streams: a global perspective. Rev. Geophys. 55 (2), 560–585. https://doi.org/10.1002/2016RG000547.

Masuda, S., Sano, I., Hojo, T., Li, Y.Y., Nishimura, O., 2018. The comparison of greenhouse gas emissions in sewage treatment plants with different treatment processes. Chemosphere 193, 581–590. https://doi.org/10.1016/j.chemosphere.2017.11.018.

Maurice, L., Rawlins, B.G., Farr, G., Bell, R., Gooddy, D.C., 2017. The Influence of Flow and Bed Slope on Gas Transfer in Steep Streams and Their Implications for Evasion of CO2. J. Geophys. Res. Biogeosciences 122 (11), 2862–2875. https://doi.org/10.1002/2017JG004045.

Mizukawa, A., Filipp, T.C., Peixoto, L.O.M., Scipioni, B., Leonardi, I.R., de Azevedo, J.C. R., 2019. Caffeine as a chemical tracer for contamination of urban rivers. Brazilian J. Water Resour.

Natchimuthu, S., Wallin, M.B., Klemedtsson, L., Bastviken, D., 2017. Spatio-temporal patterns of stream methane and carbon dioxide emissions in a hemiboreal catchment in Southwest Sweden. Sci. Rep. 7 (November 2016), 1–12. https://doi.org/10.1038/srep39729.

Natural Scotland: The river basin management plan for the Scotland river basin district 2009–2015. [online] Available from: https://www.sepa.org.uk/media/163445/the-river-basin-management-plan-for-the-scotland-river-basin-district-2015-2027.pdf, 2015.

Neal, C., Kirchner, J.W., 2000. Sodium and chloride levels in rainfall, mist, streamwater and groundwater at the Plynlimon catchments, mid-Wales : inferences on hydrological and chemical controls. Hydrol. Earth Syst. Sci. 4 (2).

Nedwell, D.B., Dong, L.F., Sage, A., Underwood, G.J.C., 2002. Variations of the nutrients loads to the mainland U.K. estuaries: correlation with catchment areas, urbanization and coastal eutrophication. Estuar. Coast. Shelf Sci. 54 (6), 951–970. https://doi.org/10.1006/ecss.2001.0867.

Nijman, T.P.A., Amado, A.M., Bodelier, P.L.E., Veraart, A.J., 2022. Relief of phosphate limitation stimulates methane oxidation. Front. Environ. Sci. 10 (April), 1–8. https://doi.org/10.3389/fenvs.2022.804512.

O'Keeffe, J., Akunna, J., Olszewska, J., Bruce, A., May, L., Allan, R., 2015. Practical measures for reducing phosphorus and faecal microbial loads from onsite wastewater treatments systems discharged to the environement. A Rev. 52.

Ockenden, M.C., Deasy, C., Quinton, J.N., Bailey, A.P., Surridge, B., Stoate, C., 2012. Evaluation of field wetlands for mitigation of diffuse pollution from agriculture: sediment retention, cost and effectiveness. Environ. Sci. Policy 24, 110–119. https://doi.org/10.1016/j.envsci.2012.06.003.

Ordnance Survey: OS open rivers, OS open rivers [online] Available from: https://www.ordnancesurvey.co.uk/business-government/products/open-map-rivers, 2022.

Phillips, B.M., Mccalla Fuller, L.B., Siegler, K., Deng, X., Tjeerdema, R.S., 2022. Treating agricultural runoff with a mobile carbon filtration unit. Arch. Environ. Contam. Toxicol. 82 (4), 455–466. https://doi.org/10.1007/s00244-022-00925-8.

Pohle, I., Baggaley, N., Palarea-albaladejo, J., Stutter, M., Glendell, M., 2021. A framework for assessing concentration-discharge catchment behavior from low-frequency water quality data. Water Resour. Res. https://doi.org/10.1029/2021WR029692.

Raymond, P.A., Hartmann, J., Lauerwald, R., Sobek, S., McDonald, C., Hoover, M., Butman, D., Striegl, R., Mayorga, E., Humborg, C., Kortelainen, P., Dürr, H., Meybeck, M., Ciais, P., Guth, P., 2013. Global carbon dioxide emissions from inland waters. Nature 503 (7476), 355–359. https://doi.org/10.1038/nature12760.

Riley, A.L., Mayes, W.M., 2015. Long-term evolution of highly alkaline steel slag drainage waters. Environ. Monit. Assess. 187 (7) https://doi.org/10.1007/s10661-015-4693-1.

Rosamond, M.S., Thuss, S.J., Schiff, S.L., 2012. Dependence of riverine nitrous oxide emissions on dissolved oxygen levels. Nat. Geosci. 5 (10), 715–718. https://doi.org/10.1038/ngeo1556.

Rosentreter, J.A., Borges, A.V., Deemer, B.R., Holgerson, M.A., Liu, S., Song, C., Melack, J., Raymond, P.A., Duarte, C.M., Allen, G.H., Olefeldt, D., Poulter, B., Battin, T.I., Eyre, B.D., 2021. Half of global methane emissions come from highly variable aquatic ecosystem sources. Nat. Geosci. 14 (4), 225–230. https://doi.org/10.1038/s41561-021-00715-2.

Salgado, J., Duc`, T.A., Nga, D.T., Panizzo, V.N., Bass, A.M., Zheng, Y., Taylor, S., Roberts, L.R., Lacey, J.H., Leng, M.J., McGowan, S., 2022. Urbanization and seasonality strengthens the CO2 capacity of the red river delta, Vietnam. Environ. Res. Lett. 17 (10) https://doi.org/10.1088/1748-9326/ac9705.

Scottish Environment Protection Agency: SEPA water level data, [online] Available from: https://www2.sepa.org.uk/WaterLevels/(Accessed 23 April 2020), 2020.

Seitzinger, S.P., Kroeze, C., 1998. Global distribution of nitrous oxide production and N inputs in freshwater and coastal marine ecosystems. Glob. Biogoehem. Cycles 12 (1), 93–113.

SEPA: Riparian vegetation management, engineering in the water environment, Good Practice Guide, 2, 1–47, 2009.

SEPA: Water enviornment hub, [online] Available from: https://www.sepa.org.uk/data-visualisation/water-environment-hub/?riverbasindistrict=Scotland, 2018.

Stets, E.G., Butman, D., McDonald, C.P., Stackpoole, S.M., DeGrandpre, M.D., Striegl, R. G., 2017. Carbonate buffering and metabolic controls on carbon dioxide in rivers. Global Biogeochem. Cycles 31 (4), 663–677. https://doi.org/10.1002/2016GB005578.

Tye, A.M., Williamson, J.L., Jarvie, H.P., Dise, N.B., Lapworth, D.J., Monteith, D., Sanders, R., Mayor, D.J., Bowes, M.J., Bowes, M., Burden, A., Callaghan, N., Farr, G., Felgate, S.L., Gibb, S., Gilbert, P.J., Hargreaves, G., Keenan, P., Kitidis, V., Jürgens, M.D., Martin, A., Mounteney, I., Nightingale, P.D., Pereira, M.G., Olszewska, J., Pickard, A., Rees, A.P., Spears, B., Stinchcombe, M., White, D., Williams, P., Worrall, F., Evans, C.D., 2022. Dissolved inorganic carbon export from rivers of Great Britain : spatial distribution and potential catchment-scale controls. J. Hydrol. 615 (PA), 128677 https://doi.org/10.1016/j.jhydrol.2022.128677.

UK Centre for Ecology & Hydrology (UKCEH): National river flow archive, [online] Available from: https://nrfa.ceh.ac.uk/data/station/info/84007, 2010.

UK Centre for Ecology & Hydrology (UKCEH): Land cover map 2015, [online] Available from: https://www.ceh.ac.uk/services/land-cover-map-2015, 2020.

UK Centre of Ecology & Hydrology (UKCEH): National river flow archive, [online] Available from: https://nrfa.ceh.ac.uk/(Accessed 5 September 2020), 2020.

Vaughan, M.C.H., Schroth, A.W., 2019. Shining light on the storm : in-stream optics reveal hysteresis of dissolved organic matter character. Biogeochemistry 143 (3), 275–291. https://doi.org/10.1007/s10533-019-00561-w.

Vaughan, M.C.H., Bowden, W.B., Shanley, J.B., Vermilyea, A., Sleeper, R., Gold, A.J., Pradhanang, S.M., Inamdar, S.P., Levia, D.F., Andres, A.S., Birgand, F., Schroth, A. W., 2017. High-frequency dissolved organic carbon and nitrate measurements reveal differences in storm hysteresis and loading in relation to land cover and seasonality. Water Resour. Res. 5345–5363. https://doi.org/10.1002/2017WR020491. Received.

Vesper, D.J., Moore, J.E., Adams, J.P., 2016. Inorganic carbon dynamics and CO2 flux associated with coal-mine drainage sites in Blythedale PA and Lambert WV, USA. Environ. Earth Sci. 75 (4), 1–14. https://doi.org/10.1007/s12665-015-5191-z.

Wang, G., Xia, X., Liu, S., Zhang, L., Zhang, S., Wang, J., Xi, N., Zhang, Q., 2021. Intense methane ebullition from urban inland waters and its significant contribution to greenhouse gas emissions. Water Res 189, 116654. https://doi.org/10.1016/j.watres.2020.116654.

Williams, C.J., Frost, P.C., Morales-williams, A.M., Larson, J.H., Richardson, W.B., Chiandet, A.S., Xenopoulos, M.A., 2016. Human activities cause distinct dissolved organic matter composition across freshwater ecosystems. Glob. Chang. Biol. 613–626. https://doi.org/10.1111/gcb.13094.

Winterdahl, M., Wallin, M.B., Karlsen, R.H., Laudon, H., Öquist, M., Lyon, S.W., 2016. Decoupling of carbon dioxide and dissolved organic carbon in boreal headwater streams. J. Geophys. Res. Biogeosciences 121 (10), 2630–2651. https://doi.org/10.1002/2016JG003420.

Wrage, N., Velthof, G.L., Van Beusichem, M.L., Oenema, O., 2001. Role of nitrifier denitrification in the production of nitrous oxide. Soil Biol. Biochem. 33 (12–13), 1723–1732. https://doi.org/10.1016/S0038-0717(01)00096-7.

Zarnetske, J.P., Haggerty, R., Wondzell, S.M., Baker, M.A., 2011. Dynamics of nitrate production and removal as a function of residence time in the hyporheic zone. J. Geophys. Res. 116 (March 2010), 1–12. https://doi.org/10.1029/2010JG001356.

Zhang, W., Yan, C., Shen, J., Wei, R., Gao, Y., Miao, A., Xiao, L., Yang, L., 2019. Characterization of aerobic denitrifying bacterium pseudomonas mendocina strain

GL6 and its potential application in wastewater treatment plant effluent. Int. J. Environ. Res. Public Health 16 (3). https://doi.org/10.3390/ijerph16030364.
Zhang, W., Li, H., Xiao, Q., Li, X., 2021. Urban rivers are hotspots of riverine greenhouse gas (N2O, CH4, CO2) emissions in the mixed-landscape chaohu lake basin. Water Res 189, 116624. https://doi.org/10.1016/j.watres.2020.116624.
Zhou, Y., Toyoda, R., Suenaga, T., Aoyagi, T., Hori, T., 2022a. Low nitrous oxide concentration and spatial microbial community transition across an urban river affected by treated sewage. Water Res 216 (February), 118276. https://doi.org/10.1016/j.watres.2022.118276.
Zhou, Y., Toyoda, R., Suenaga, T., Aoyagi, T., Hori, T., 2022b. Low nitrous oxide concentration and spatial microbial community transition across an urban river affected by treated sewage. Water Res 216 (February), 118276. https://doi.org/10.1016/j.watres.2022.118276.
Stanley, E.H., Casson, N.J., Christel, S.T., Crawford, J.T., Loken, L.C., Oliver, S.K, 2016. The ecology of methane in streams and rivers: Patterns, controls, and global significance. Ecol. Monogr. 86 (2), 146–171. https://doi.org/10.1890/15-1027.
Billett, M.F., Moore, T.R., 2008. Supersaturation and evasion of CO2 and CH4 in surface waters at Mer Bleue peatland, Canada. Hyrdological Process 22, 2044–2054. https://doi.org/10.1002/hyp.